Co-option of immune effectors by the hormonal signalling system triggering metamorphosis in *Drosophila melanogaster*

Catarina Nunes[1*], Takashi Koyama[2], Élio Sucena[1,3*]

[1] Evolution and Development Laboratory, Instituto Gulbenkian de Ciência, Oeiras, Portugal
[2] Section for Cell and Neurobiology, Department of Biology University of Copenhagen, Copenhagen, Denmark
[3] Departamento de Biologia Animal, Faculdade de Ciências, Universidade de Lisboa, Lisbon, Portugal
* Corresponding authors: cdnunes@igc.gulbenkian.pt (CN); esucena@igc.gulbenkian.pt (ES)

Running title: Hormonal control of immunity at metamorphosis

Keywords: Ecdysone, Anti-Microbial Peptides (AMP), Insect Metamorphosis, Drosomycin

Abstract

Insect metamorphosis is regulated by the production, secretion and degradation of two peripheral hormones: 20-hydroxyecdysone (ecdysone) and juvenile hormone (JH). In addition to their roles in developmental regulation, increasing evidence suggests that these hormones are involved in innate immunity processes, such as phagocytosis and the induction of antimicrobial peptide (AMP) production. AMP regulation includes systemic responses as well as local responses at surface epithelia that contact with the external environment. At pupariation, *Drosophila melanogaster* increases dramatically the expression of three AMP genes, *drosomycin (drs)*, *drosomycin-like 2 (drsl2)* and *drosomycin-like 5 (drsl5)*. We show that the systemic action of *drs* at pupariation is dependent on ecdysone signalling in the fat body and operates via the ecdysone downstream target, Broad-Z4. In parallel, ecdysone also regulates local responses, specifically through the activation of *drsl2* expression in the gut. Finally, we confirm the relevance of this ecdysone dependent AMP expression for the control of bacterial persistence by showing that flies lacking *drs* expression in the fat body have higher bacterial persistence over metamorphosis. Together, our data emphasize the importance of the association between ecdysone signalling and immunity using *in vivo* studies and establish a new role for ecdysone at pupariation, which impacts developmental success by regulating the immune system in a stage-dependent manner. We speculate that this co-option of immune effectors by the hormonal system may constitute a pre-emptive mechanism to control bacterial numbers in the pupa at the core of metamorphosis evolution.

33 # Introduction

34 Insect development and physiology are mainly regulated by two peripheral hormones:
35 the steroid hormone, 20-hydroxyecdsyone (hereafter, ecdysone) and the sesquiterpenoid
36 hormone, juvenile hormone (JH) (1,2). In vertebrates, steroid hormones and their nuclear
37 receptors are key regulators of systemic immune responses, namely through the enhancement
38 of inflammation (3). Similarly, in insects, steroid hormones are also known to be involved in
39 innate immunity (4–9). Ecdysone titre is tightly regulated to control developmental transitions
40 and as such, steroid hormone-dependent activation of innate immunity seems appropriate for
41 stage-specific regulation of immunity.
42 When in contact with a microorganism, insects rely on the activation of three tightly
43 related immunity processes: i) cellular immunity (i.e. phagocytosis and encapsulation of
44 invading microorganisms); ii) the induction of proteolytic cascades, that culminate in
45 melanisation; and iii) production of antimicrobial peptides (AMPs), which is primarily
46 regulated at the transcriptional level through two distinct signalling pathways, Toll and Imd,
47 triggered by sensing of Lys-type peptidoglycan and β-1,3-glucan or meso-diaminopimelic
48 acid (DAP)-type peptidoglycan, respectively (10–12). In insects with complete
49 metamorphosis (holometabolans), AMP genes are usually silent in the absence of an immune
50 challenge and their expression is induced upon injury and/or infection (13). However, indirect
51 evidence suggests that AMPs may be up-regulated at specific developmental stages
52 irrespective of pathogen presence. Studies in the moth *Manduca sexta* show that expression of
53 lysozyme and of the AMPs *cecropin A*, *cecropin B* and *hemolin* increases dramatically during
54 metamorphosis, although it is not clear what regulates this increase and its role(s) *in vivo* (14–
55 16). This transcriptional AMP peak occurs before the end of histolysis of the larval midgut,
56 that is, before cells are potentially exposed to any pathogen or bacterium. In this context, the
57 accumulation of AMPs at the end of the feeding stage may constitute a first response against
58 the possible harmful effects to the pupa of expanding bacteria carried-over from the gut
59 remodelling process (17–20). Nonetheless, studies in dipterans show that some species of
60 bacteria in the larval gut can persist inside the host throughout metamorphosis (19–22). In
61 *Drosophila melanogaster,* RNAseq analysis revealed a peak in the expression of AMPs at
62 pupariation, of which around 95% consists of three AMPs: *drs*, *drosomycin-like 2 (drsl2)* and
63 *drosomycin-like 5 (drsl5)* (23). Furthermore, five different AMPs (*diptericin, drs, attacin-A,*
64 *metchnikowin* and *cecropin A1*) are shown to contain putative *cis*-regulatory elements for
65 potential binding of the functional ecdysone receptor complex, suggesting an ecdysone-
66 dependent control of their expression (24). Importantly, the compelling association between

67 ecdysone signalling and immunity at this particular stage of development is not restricted to
68 the humoral arm of the immune response. An ecdysone-dependent increase in phagocytic
69 capacity of plasmatocytes at pupariation has been described and hypothesized to be
70 particularly important given the higher predisposition for infection at the pupal stage (6).
71 Considering the above, we hypothesized that ecdysone signalling controlling
72 development was co-opted to regulate the expression of AMPs at pupariation. Previous *in*
73 *vitro* study has shown that ecdysone promotes humoral immunity by increasing the
74 expression of AMP genes, such as *diptericin, cecropin* and *attacin,* via the EcR-USP receptor
75 complex in S2 cells (5). In addition, a microarray analysis of 20E-treated S2 cells revealed the
76 existence of two distinct mechanisms for 20E-regulated AMP expression: one in which the
77 critical step is the activation of peptidoglycan recognition protein (PGRP)-LC - a critical
78 pattern recognition receptor (PRR) of the Imd pathway - by ecdysone for controlling the
79 expression of *cecropin A1, attacin-A and defensin*; and another, in which the hormonally-
80 controlled mechanism is absolutely required for the expression of *drs, metchnikowin* and
81 *diptericin* (4). However, the importance of the requirement of ecdysone for the expression of
82 AMPs, and its role, nor the regulatory mechanism through which this hormone affects innate
83 immunity have been explored.
84 In this study, we demonstrate that ecdysone regulates the expression of AMPs *in vivo*
85 at pupariation, both systemically (by regulating the expression of *drs*) and locally in the
86 midgut (by regulating the expression of *drsl2*). Importantly, the systemic expression of *drs*
87 has an impact on the number of bacteria that persists and proliferates during metamorphosis,
88 corroborating the hypothesis that the AMP peak has a function in controlling bacteria during
89 metamorphosis. Furthermore, we show that this association between the expression of *drs* and
90 ecdysone in the absence of infection occurs solely at pupariation and through the early
91 ecdysone-response gene Broad-Z4, which is only expressed at the end of the feeding stage
92 (25). Taken together, our findings fill a gap in current knowledge by shedding light onto the
93 mechanisms and biological significance of hormonal control of humoral immunity at
94 metamorphosis with potential evolutionary importance.

95 Results

96 <u>*drs, drsl2* and *drsl5* are expressed at pupariation in a bacteria-independent manner</u>

97 Around 95% of the anti-microbial peptide (AMP) peak at pupariation, mentioned
98 above (23), consists of three AMPs: *drs, drsl2* and *drsl5* (Supplementary Figure 1). Upon gut

99 remodelling at metamorphosis, an ineffective gut purge could lead to the canonical activation
100 of immunity pathways, resulting in a peak of AMP expression. To test if the presence of
101 bacteria constitutes the trigger for the expression of *drs, drsl2* and *drsl5*, we performed real-
102 time quantitative PCR (qPCR) in mid-L3 larvae (L3) and newly pupariated (P0) samples of
103 germ-free (GF) or standardly-raised individuals. We confirmed that expression increases at
104 pupariation for all AMPs tested (Figure 1, S1 table, Supplementary Figure 2), including *drs*
105 *(lsmean, pairwise~{w-};+;+ | Stage*drs<0.0001), drsl2*
106 *(lsmeans(pairwise~{w};+;+|Stage*drsl2 <0.0001))* and *drsl5 (lsmeans(pairwise~{w-*
107 *};+;+|Stage*drsl5<0.000))*. This increment is not lost under GF conditions with the putative
108 exceptions of *cecropinA1* and *defensin*. Importantly, the three main AMPs under scrutiny,
109 *drs, drsl2* and *drsl5*, show a marked independence of the presence of microbes, including
110 yeast, for their expression at this developmental transition
111 (*lsmeans(pairwise~{w};+;+|Stage*drs <0.0001); lsmeans(pairwise~{w-};*
112 *+;+|Stage*drsl2<0.0001); lsmeans(pairwise~{w};+;+|Stage*drsl5 <0.0001))* (Figure 1, S1
113 table). In turn, this is not the case for other AMPs, such as for example *cecropinA1* or
114 *defensin*, which show decreased expression in the absence of gut bacteria (Supplementary
115 Figure 2, S1 table).
116

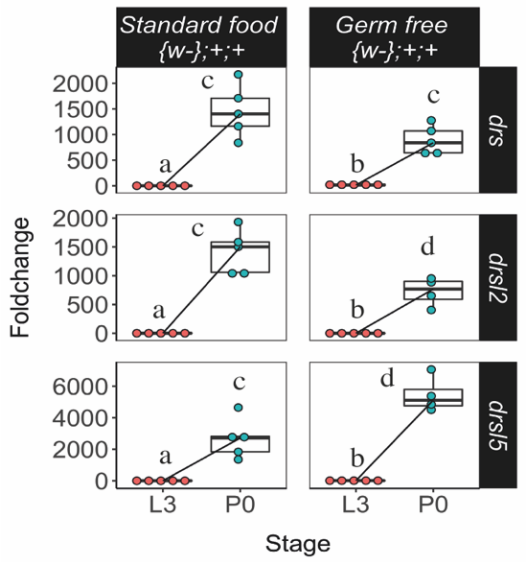

117

118 **Figure 1. Expression of *drs*, *drsl2* and *drsl5* is independent of bacterial presence.** The expression
119 levels of *drs, drsl2* and *drsl5* increase at pupariation and are not lost under GF conditions. Different letters
120 represent statistically significant differences in foldchange. Foldchange was determined using the ΔΔCT method.
121

Together, these results reject the hypothesis that expression of the three main AMPs at pupariation is dependent on microbial induction and suggest that it may be hardwired to the developmental programme.

Ecdysone regulates the expression of *drs*

We focused primarily on two main sources of AMP expression with systemic action, the fat body and haemocytes (12). We manipulated ecdysone signalling sensitivity in these tissues, simultaneously and specifically, to ensure no perturbation of normal development and pupariation timing. For that we used *Cg-Gal4* combined with a *tub-Gal80[ts]*, a thermo-sensitive allele of *Gal80* under the control of the tubulin promoter (hereafter *Cg[ts]*), to drive the expression of a dominant negative ecdysone receptor under the control of the UAS sequence (26) *(EcR-A DN W650A TP3*, hereafter *EcRDN*). The reduction of ecdysone sensitivity was triggered from the onset of L3 or at wandering stage, and resulted in the elimination of the *drs* peak at P0, compared to control conditions (Figure 2A, (*lsmeans(pairwise~Stage|Cg[ts]>mcD8GFP)=0.0001*, lsmeans(pairwise~Stage|*Cg[ts]>EcRDN)* =0.0017, lsmeans(pairwise~Genotype|P0) <0.0001)). However, the expression of *drsl2* and *drsl5* (Figure 2A, S2 Table) and of the other AMPs (Supplementary Figure 3-1, S2 Table) was not eliminated. Furthermore, *drs* expression still increases in mutant flies for *dif,* the NF-κB factor that triggers *drs* expression upon activation of the Toll pathway (Supplementary Figure 3-2, lsmeans(pairwise~Stage|*{w-};+;+*<0.0001, *lsmeans(pairwise~Stage|{w-};dif1;+)*<0.0001, *lsmeans(pairwise~Genotype|P0)= 0.0703*)), suggesting that the expression of *drs* at pupariation is partially independent of the action of the NF-κB factor.

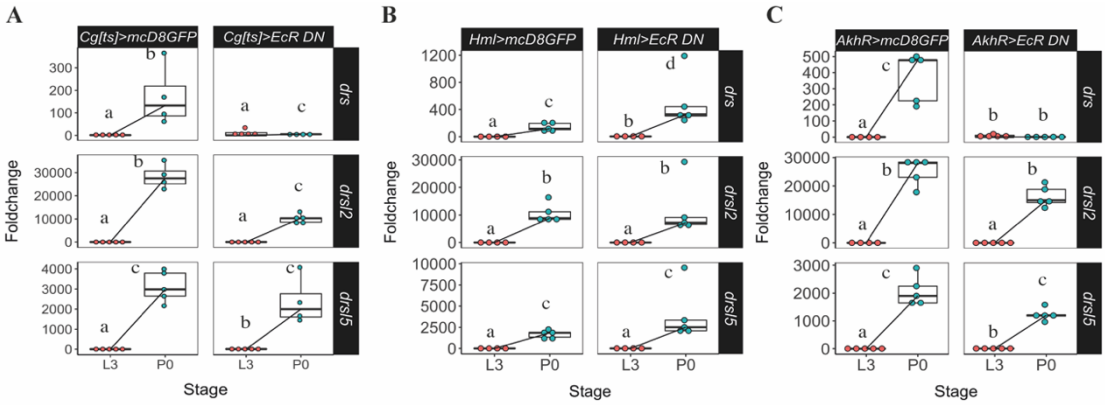

147 **Figure 2. Expression of drs at pupariation is developmentally regulated by ecdysone in the fat**
148 **body.** (A) Foldchange increase in drs expression (but not of *drsl2* or *drsl5*) at pupariation was eliminated when
149 ecdysone sensitivity is decreased specifically in the fat body and haemocytes simultaneously. (B) Reduced
150 ecdysone sensitivity in the haemocytes does not affect the expression of the AMPs under study. (C) Reduced
151 ecdysone signalling in the fat body resulted in decreased *drs* expression at pupariation
152 (lsmeans(pairwise~Stage|AkhR>mcD8GFP <0.0001, lsmeans(pairwise~Stage|AkhR>EcRDN)=0.6709), without
153 affecting the expression of *drsl2* and *drsl5* (lsmeans (pairwise~Stage|AkhR>mcD8GFP)<0.0001,
154 lsmeans(pairwise~Stage|AkhR>EcRDN) <0.0001), for both genes). Different letters represent statistically
155 significant differences in foldchange. Foldchange was determined using the ΔΔCT method.

156

157 This result was further confirmed by targeting haemocytes and fat body
158 independently, using the specific drivers *Hemolectin-Gal4* (*Hml-ΔGal4*) for the haemocytes
159 and *Adipokinetic hormone receptor-Gal4* (*AkhR-Gal4)* for the fat body. When ecdysone
160 sensitivity was reduced in the haemocytes, expression of *drs*, *drsl2* and *drsl5,* as well as of
161 other four AMPs, was unaffected (*lsmeans(pairwise~Stage|Hml>mcD8GFP)<0.0001*,
162 *lsmeans(pairwise~Stage|Hml>EcR DN)<0.0001*), for the three genes), (Figure 2B and
163 Supplementary Figure 3-3, S3 Table). However, although reduced ecdysone sensitivity in the
164 fat body (*AkhR>EcRDN*) did not affect the expression of *drsl2* and *drsl5* (Figure 2C,
165 (*lsmeans(pairwise~Stage|AkhR >mcD8GFP) <0.0001*, *lsmeans*
166 *(pairwise~Stage|AkhR>EcRDN)<0.0001),* for both genes) or of other AMPs (Supplementary
167 Figure 3-4 , S4 Table), it resulted in decreased expression of *drs* at pupariation. (Figure 2C,
168 *lsmeans(pairwise~Stage|AkhR>mcD8GFP) <0.0001, lsmeans(pairwise~Stage|AkhR*
169 *>EcRDN) =0.6709*). It is noteworthy to mention that this reduction of *drs* expression is not
170 likely due to the EcR-mediated disruption of fat body metabolism or abnormal developmental
171 effects because most of the AMP gene expression was not altered.
172 Altogether, these results indicate that *drs* expression - but not *drsl2* or *drsl5* - is
173 systemically regulated by ecdysone signalling specifically in the fat body at pupariation.

174 <u>Expression of *drsl2* in the midgut is regulated by Ecdysone</u>

175 Having determined that the expression of *drsl2* and *drsl5* is developmentally
176 regulated but does not involve the fat body, we turned our attention to two of the most
177 important tissues for local immune response: the epithelial layers of the gut and trachea (27).
178 First, we overexpressed *EcRDN* specifically in the most abundant cells of the midgut, the
179 enterocytes, using the specific driver *Mex-Gal4* (*Mex>EcRDN*). Unlike the fat body, the gut is
180 not responding to the pupariation ecdysone pulse by increasing *drs* expression (Figure 3A). In
181 contrast, decreased ecdysone sensitivity specifically in the midgut resulted in a drastic

182 reduction (*circa* 600-fold) of *drsl2* expression, very close to the L3 basal levels (Figure 3A),
183 *lsmeans(pairwise~Genotype|P0)<0.0001; lsmeans(pairwise~Stage|Mex> EcRDN)*
184 *<0.0001*)).
185

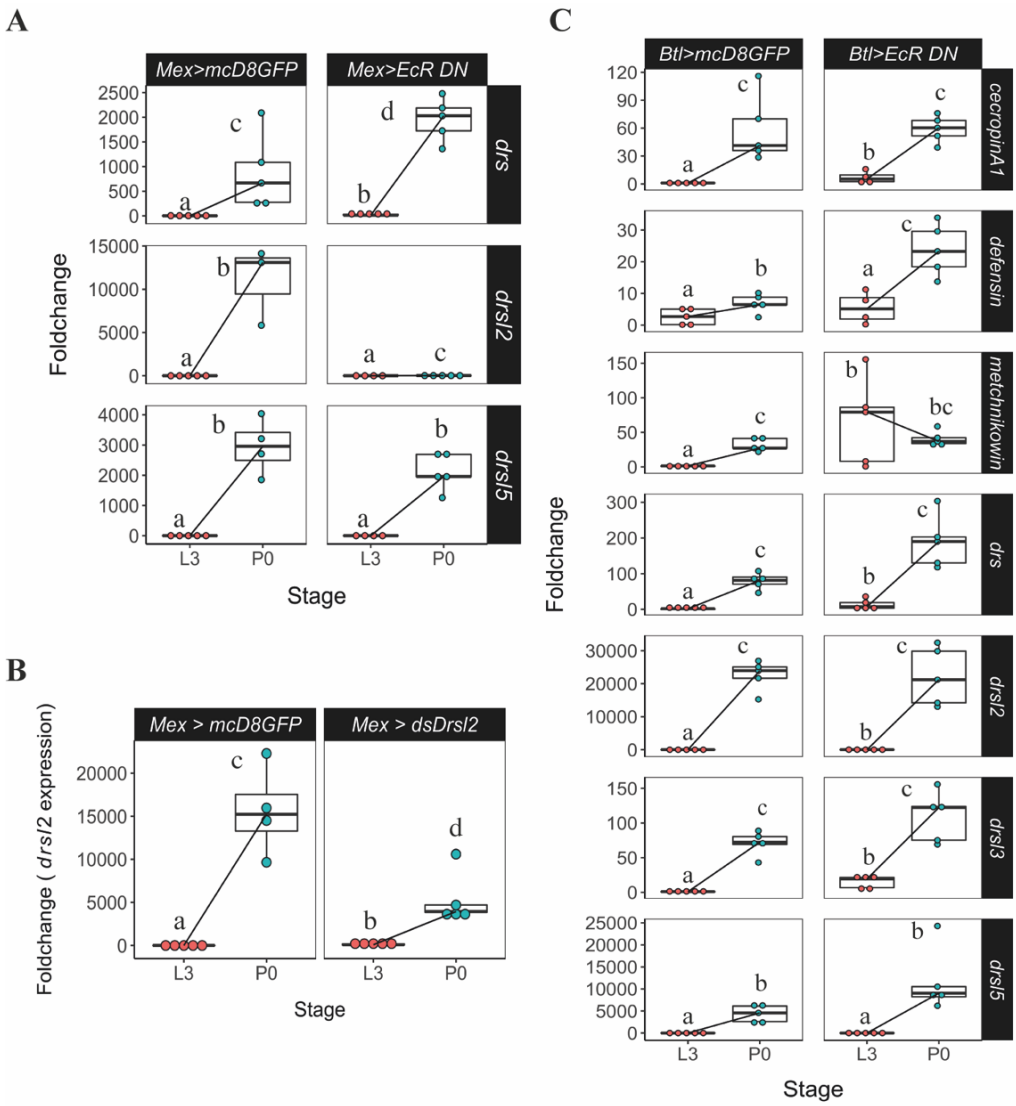

186
187 **Figure 3. Gut and tracheal expression of relevant AMPs.** (A) Manipulation of ecdysone sensitivity
188 specifically in the midgut reduced the expression of *drsl2*, but not of *drs* or *drsl5*. (B) Knock-down of *drsl2*
189 specifically in the midgut resulted in an overall decrease in the expression of this AMP. Each dot represents a
190 sample of five pooled individuals; the lines connect the median of the samples at L3 and P0. (C) Ecdysone
191 signalling in the trachea does not affect the expression of any AMP under study. Different letters represent
192 statistically significant differences in foldchange. Foldchange was determined using the ΔΔCT method.
193
194 We further confirmed this result by inducing RNAi (through the expression of double
195 stranded RNA for *drsl2* under UAS control) and consequent knock-down of *drsl2* specifically
196 in the midgut (*Mex>ds-drsl2*). This resulted in an overall decrease in the expression of this

197 AMP at pupariation (Figure 3B, *lsmeans(pairwise~Genotype|P0)<0.0237;*
198 *lsmeans(pairwise~Stage|Mex>ds-drsl2) <0.0001*), which indicates that the midgut is a source
199 of the ecdysone-dependent production of *drsl2* at this stage. Interestingly, we failed again to
200 detect any difference in the expression of *drsl5*, one of the three main players in the AMP
201 ecdysone-dependent peak (Figure 3A, *lsmeans (pairwise~Genotype|P0)<0.4479;*
202 *lsmeans(pairwise~Stage|Mex>EcRDN)<0.0001*), S5 table). However, other tested AMPs also
203 appear to be, at least partially, regulated by ecdysone signalling in the midgut at pupariation.
204 Under ecdysone-signalling down-regulation conditions, significant decrease in
205 mRNA levels were observed for: *cecropin A1* (*lsmeans(pairwise~Genotype|P0) <0.0001;*
206 *lsmeans(pairwise~Stage|Mex>EcRDN)=0.0038), defensin (lsmeans*
207 *(pairwise~Genotype|P0)<0.0001; lsmeans(pairwise~Stage|Mex>EcR*
208 *DN)=0.3866*),*metchnikowin* (*lsmeans(pairwise~Genotype|P0)=0.0060; lsmeans*
209 *(pairwise~Stage|Mex>EcRDN<0.0001*), and *drsl3((lsmeans(pairwise~Genotype|P0)*
210 *=0.0008;lsmeans(pairwise~Stage|Mex>EcRDN)=0.2084*), Supplementary Figure 4).
211 On the other hand, decreased ecdysone sensitivity in the trachea, using the specific
212 driver *btl*-Gal4 (*btl>EcRDN*), did not have an impact on the expression of any of the three
213 major AMPs under study (Figure 3C, S6 Table). These results show that a layer of local AMP
214 action is at play through the sensing of the ecdysone peak at the onset of pupariation in the
215 gut epithelium.
216 Together the local and systemic mechanisms of action that share ecdysone control,
217 consisting of *drsl2* and *drs*, account for about 70% of the pupariation AMP peak.
218 Contrastingly, the data also point towards an alternative mechanism for regulating the
219 expression of *drsl5* at pupariation, which is either independent of ecdysone or is regulated by
220 this hormone in an alternative tissue or cell type that were not tested.

221 Br is involved in systemic *drs* induction through the fat body at pupariation

222 Next, we focused our efforts in trying to uncover more of the molecular regulation of
223 *drs* expression, the systemic arm of this ecdysone co-opted immune action.
224 Previous RNAseq data showed that the expression of *drs* markedly increases at
225 pupariation and gradually drops the expression in next 24 hours (Supplementary Figure 1,
226 (23)). We further confirmed that the expression of *dhr3* (a gene directly regulated by the
227 ecdysone-ecdysone receptor complex) and that of *drs* are tightly correlated and peak
228 exclusively at pupariation (Figure 4A). Importantly, this robust expression of *drs* at the onset

229 of metamorphosis seems to be a general feature regardless of their genetic background
230 (Supplementary Figure 5-1).
231

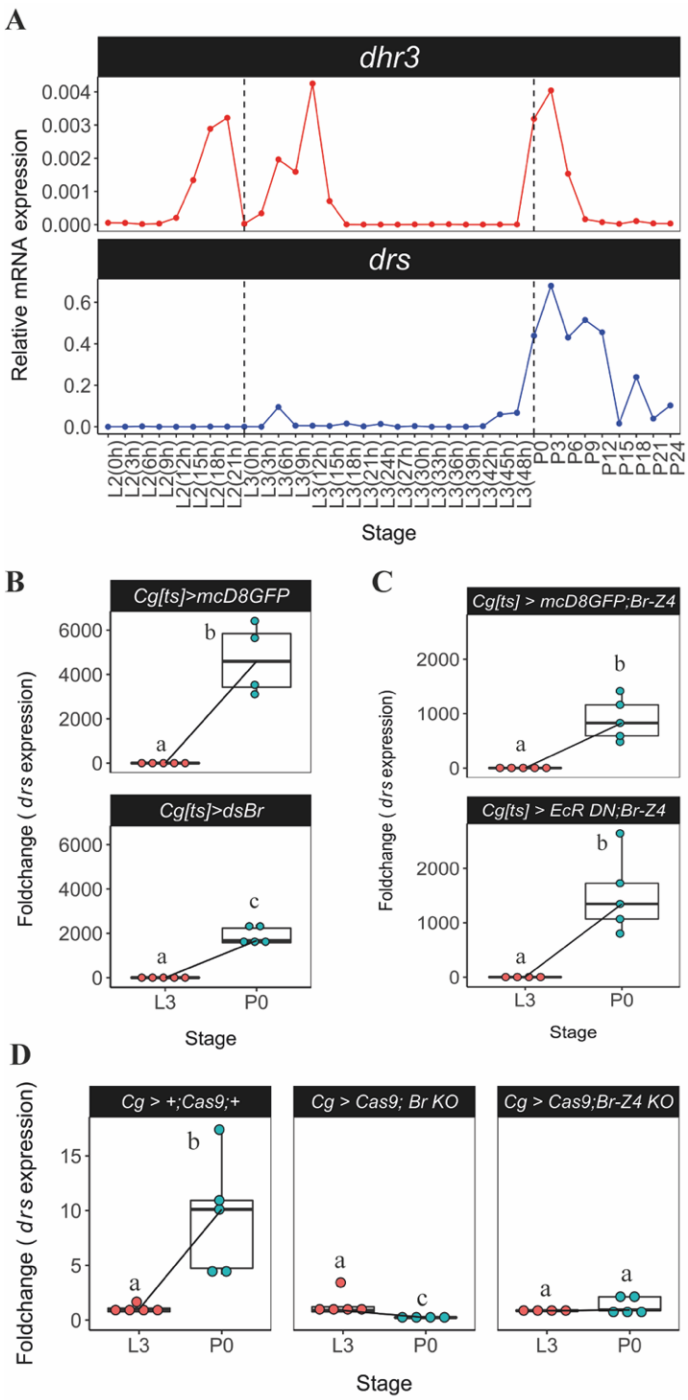

232
233
234
235

236 **Figure 4. Ecdysone signalling regulates fat body expression of *drs* at pupariation via Br-Z4. (A)**
237 *drs* expression is temporally correlated with a proxy of ecdysone activity, *dhr3*. Samples of *D. melanogaster* larvae
238 and pupae were precisely staged at the onset of the instars and collected every 3h. The expression of *dhr3* and *drs*
239 was determined by qPCR for each timepoint. Dashed black lines represent the moult to the L3 or pupariation. **(B)**
240 Knockdown of *br* specifically in the fat body and haemocytes leads to decreased expression of *drs* at P0. (**C**) Co-
241 overexpression of *br-Z4* when ecdysone sensitivity is decreased in the fat body and haemocytes is sufficient to
242 rescue the expression of *drs* at pupariation (**D**) Conditional CRISRP-mediated knock-outs for the common region
243 of *br* and *br-Z4* lead to loss of *drs* expression at pupariation. Each dot represents a sample of five pooled
244 individuals; the lines connect the median of the samples at L3 and P0; different letters represent statistically
245 significant differences in foldchange, determined using the ΔΔCT method.
246
247 *br* is a direct target of ecdysone receptor, characterized as a holometabolan pupal
248 specifier with increased expression before pupariation (25,28,29). Because the transcriptional
249 peak of *drs* is only found at the moult from the L3 to pupa but not from the L2 to L3, Br
250 seems a good candidate for regulation of the *drs* expression. We thus examined the
251 association between *br* and the ecdysone-sensitive systemic induction of *drs* at
252 metamorphosis by knocking-down *br* specifically in the fat body and haemocytes. This led to
253 a significant decrease in the expression of *drs* at pupariation, when compared to the control
254 (Figure 4B, *lsmeans(pairwise~Genotype|P0)= 0.0510*)), suggesting a role for *br* in the
255 regulation of *drs* expression. To further explore this possibility, we simultaneously reduced
256 ecdysone signalling and restored *br* in the haemocytes and fat body. This was sufficient to
257 rescue the expression of *drs* to control levels at P0 (Figure 4C,
258 *lsmeans(pairwise~Genotype|P0)= 0.3068*). Furthermore, we generated two different
259 conditional CRISPR-mediated knock-out constructs (30,31), one targeting a common region
260 to all *br* isoforms and, the other, a region specific to *br-Z4,* previously associated with AMP
261 expression using *in vitro* techniques in a different species (32). Knock-out of all *br* isoforms
262 or of *br-Z4* alone in haemocytes and fat body, led to the elimination of the *drs* peak at
263 pupariation (Figure 4D, *lsmeans(pairwise~Stage|Cg> +;Cas9;+)*
264 *<0.0001;lsmeans(pairwise~Stage| Cg>Cas9;br KO)=0.0001,*
265 *lsmeans(pairwise~Stage|Cg>Cas9;br-Z4 KO)=0.4691*, S8 table), supporting that Br is
266 involved in the regulation of *drs* expression at pupariation downstream of the ecdysone
267 receptor complex in the fat body.
268 To further explore this regulation of *drs* expression by Br-Z4, we used the JASPAR
269 (http://jaspar.genereg.net) matrix MA0013.1 to run a comprehensive search for Br-Z4 binding
270 sites over 2 kb of putative promoter region that is upstream of the coding sequence of *drs*,
271 obtained from Flybase (http://flybase.net/), using FIMO software (33) (Supplementary Figure

5-2). We identified three putative Br-Z4 binding sites (p-value<0.0001) in the predicted 5' promoter region of *drs* (Supplementary Figure 5-3).

Together, these results support the idea that Br, specifically isoform Br-Z4, is involved in the regulation of the expression of *drs* either directly or indirectly at pupariation.

drs is necessary to reduce bacteria derived from imperfect larval gut purge

Having establish the basis of the regulation of *drs* at the onset of metamorphosis, we set to determine its relevance to the control of bacterial numbers throughout pupal development. Indeed, before pupariation and metamorphosis, larvae purge their gut contents and any imperfection in this process creates the conditions in the pupa for a putatively rampant infection. Thus, we examined whether or not gut purge eliminates all bacteria from the gut and how this process may be dependent on the systemic action of Drs.

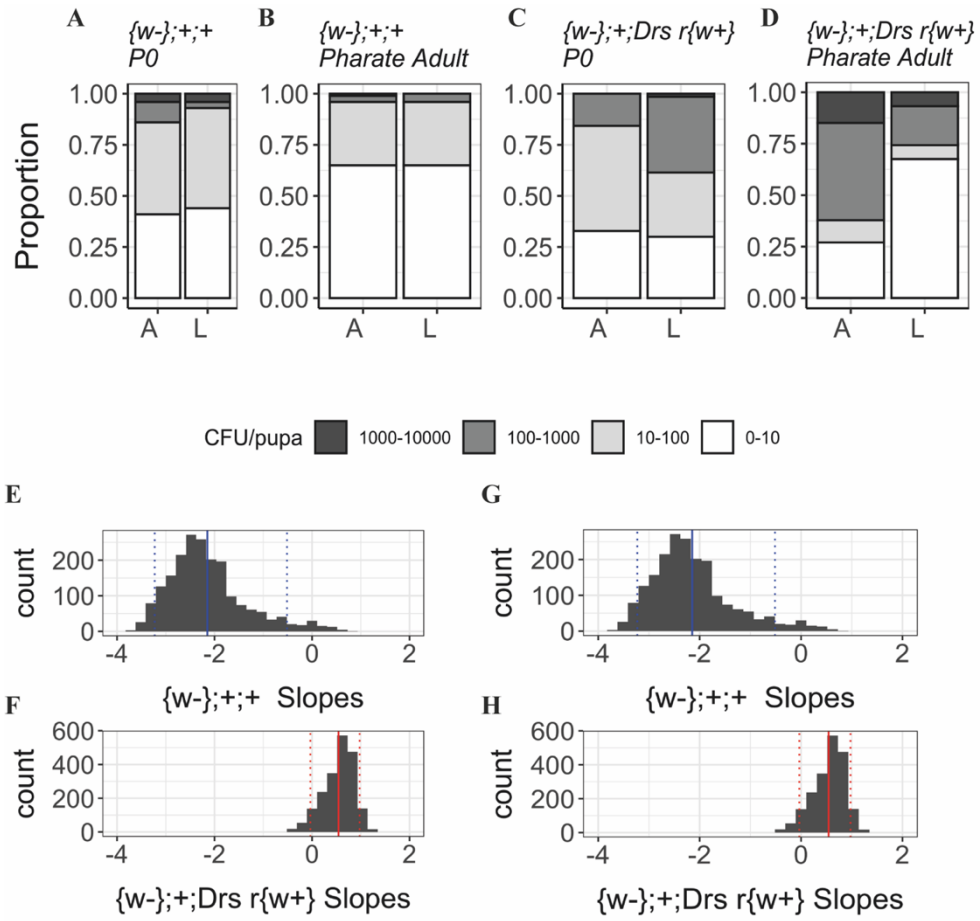

Figure 5 (A-F) Bacteria quantification (*Lactobacillus* (L) and *Acetobacter* (A)) in P0 pupae and pharate adults in wild-type and drs mutants. (A-B) In control flies *({w-};+;+)*, the number of pupae with more bacteria decreases between P0 and pharate adult stages. (C-D) In the *drs* mutant line *({w-};+; Drs r{w+}),* there are more individuals with higher loads of bacteria persisting from P0 to pharate adult. (E-F) Slopes for the number of *Lactobacillus* in control and the mutant lines. (E) Control samples have negative slopes indicating a decrease in the number of bacteria between stages. (F) *drs* mutant samples have positive slope values, representative of an increase in the number of bacteria across metamorphosis. (G-H) Slopes for the number of *Acetobacter* in the control and the mutant lines. (G) Control samples distribution show negative slopes, i.e., a decrease in the number of bacteria between stages. (H) *drs* null mutant displays positive slope values. Doted lines represent the 0.05 and 0.95 quantiles; full line represents the mean slope.

Under our standard rearing conditions, the mortality between P0 and pharate adult is negligible, which allows us to infer and correlate the bacterial numbers detected in each of these developmental stages (Supplementary Figure 6, S7 Table). After gut purge, approximately 5% of control P0 individuals contained bacteria in the order of the thousands and another 12% in the order of the hundreds (Figure 5A). However, at the pharate adult stage, the number of individuals in these two categories decreased alongside an increase in the number of individuals without detectable bacteria (Figure 5B). In contrast, *drs* null mutants showed an increase rather than a decrease in the number of pupae with more bacteria between these two stages (Figure 5C and 5D), supporting that Drs is necessary to eliminate gut derived bacteria during metamorphosis.

Using a resampling strategy, we determined that most coefficients associated with the control line were negative (Figure 5E (*Median: -2.279 (IQR: -2.682 -1.803); One-way Wilcoxon test for median<0: <2.2e-16, r= 0.864)* and Figure 5G *(Median: -2.317 (IQR: -2.907 -1.858); One-way Wilcoxon test for median<0: <2.2e-16, r=0.866*)). On the other hand, the coefficients associated with *drs* null mutant were mostly positive for both bacteria types (Figure 5F *((Median: 0.596 (IQR: 0.359; 0.757); One-way Wilcoxon test for median> 0: <2.2e-16, r= 0.845*) and Figure 5H (*Median: 2.055 (IQR: 1.897; 2.192); One-way Wilcoxon test for median> 0: <2.2e-16, r=0.866*)). These results suggest that, throughout metamorphosis, a process that is dependent on the increase of AMP expression at pupariation is necessary for controlling the persistence of bacteria originating from gut purge imperfections.

When ecdysone signalling activity is decreased in the fat body and haemocytes (*Cg[ts]>EcRDN)*, a similar pattern can be observed: there is a higher proportion of individuals with larger loads of persisting bacteria (Figure 6A-B). The resampling strategy revealed that *Cg[ts]>EcRDN* samples have positive slope values for both *Lactobacillus*

(Figure 6C, *Median: 2.746 (IQR: 2.562; 2.930); One-way Wilcoxon test for median>0: <2.2e-16, r=0.866)* and *Acetobacter* (Figure 6D, *Median: 1.981 (IQR: 1.795; 2.184); One-way Wilcoxon test for median>0: <2.2e-16, r=0.866)*, which is in accordance with increased bacterial loads during metamorphosis. Importantly, *Mex>EcRDN* individuals do not have increased bacterial loads during metamorphosis, suggesting that the local immune response does not have a measurable antibacterial effect relatively to the systemic response that is still operating in these conditions (Supplementary Figure 7).

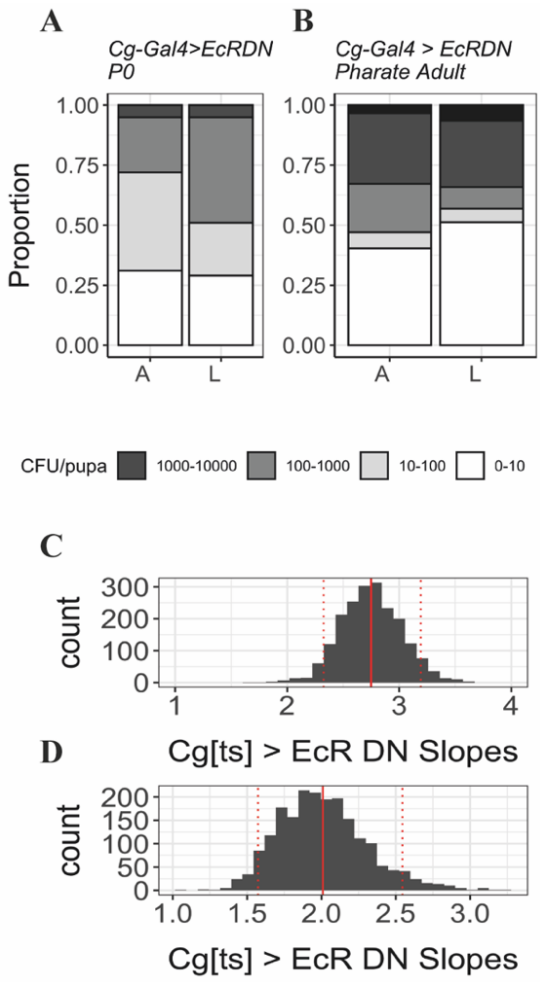

332 **Figure 6 (A-D) Quantification in P0 pupae and pharate adults of *Lactobacillus* (L) and**
333 ***Acetobacter* (A) with or without ecdysone signalling in the fat body and haemocytes.** (A-B) When
334 ecdysone sensitivity is decreased in fat body and haemocytes, the number of both bacteria types increases in P0
335 and pharate adults. Y-axis represents the proportion of individuals in each bacterial count category. (C-D)
336 Coefficient (slopes) distribution in *Cg[ts]>EcRDN* samples of *Lactobacillus* (C) and *Acetobacter* (D). Doted lines
337 represent the 0.05 and 0.95 quantiles; full line represents the mean slope.
338

339 # Discussion

340 In this study in *D. melanogaster*, we establish the association between ecdysone and
341 the increased expression of *drs* and its paralogues at pupariation and the biological
342 consequence of this process. We determine the functional link, to our knowledge yet
343 undescribed in any species, between the endocrine and immune systems, acting both
344 systemically and locally during metamorphosis to control the number of bacteria in the pupal
345 case. The biological significance of the AMP peak at the onset of metamorphosis is revealed
346 by the systemic expression of *drs*, as both mutant and ecdysone sensitivity-reduced
347 individuals showed an increase rather than a decrease in the number of bacteria between P0
348 and pharate adult stages. Interestingly the effect was detected for both Gram-positive
349 (*Lactobacillus*) and Gram-negative (*Acetobacter*) bacteria. Although Drs is generally
350 characterized as an antifungal AMP, previous studies already demonstrated that it can also be
351 induced by both Gram-positive and Gram-negative bacteria (35–41). As such, the unexpected
352 higher impact of *drs* absence on *Acetobacter* may be explained by a direct impact on Gram-
353 negative bacteria. Indeed, a previous study demonstrated that *drs* is induced in the fat body
354 after a systemic infection with *Ecc15* (34), which suggests this AMP responds to the presence
355 of Gram-negative bacteria and may be relevant under an infection scenario. Alternatively, the
356 impact seen on Gram-negative bacteria might be due to some compensatory mechanism
357 driven by other AMPs in the absence of Drs. Also of note that the humoral arm of defence is
358 not the only one acting at this stage of development. Regan and colleagues demonstrated that
359 at pupariation, ecdysone is required to activate haemocytes and to orchestrate the active
360 migration of these cells towards wounding sites (6). Therefore, at this stage both ecdysone-
361 regulated cellular and humoral mechanisms are likely to act in synergy to decrease the
362 probability of a damaging infection.
363 Surprisingly two of the actors in this process, *drsl2* and *drsl5*, have not been found to
364 have any antibacterial activity (34). However, both these AMPs are upregulated in the gut
365 upon *Erwinia carotovora* infection, which suggests that they may be relevant during an

366 immune challenge (34) and aligns with our findings. Further studies should ascertain the
367 exact mode of action of these drosomycin-like peptides.
368 Because *drsl2* and *drsl5* are not proven to act as AMPs and given that the lack of
369 local expression of *drsl2* did not affect bacterial persistence *per se*, we focused our efforts on
370 disentangling more of the molecular regulation of *drs* expression in the fat body. We showed
371 that the expression of *drs* at this stage depends upon the expression in the fat body of the
372 ecdysone receptor target, *br-Z4*. This is in accordance to previous indications that Br is
373 essential for the PGRP-LC-independent hormonal regulation of *drs* in S2 cells (4). However,
374 these previous studies did not demonstrate this association *in vivo*, thus not establishing the
375 spatial and temporal range of Br action on AMPs nor its relation to pupal viability.
376 Furthermore, similar ecdysone-mediated immune activation through Br has been previously
377 observed. Studies in the silkworm *Bombyx mori* showed that during metamorphosis, ecdysone
378 activates the transcription of lysozyme via Br-Z2 (42) and of the AMP *lebocin* via Br-Z4 (32).
379 This intermediary role of Br in the regulation mechanism of ecdysone over the AMPs
380 may explain why these effectors are only upregulated at pupariation, as revealed by our
381 expression profile data. Although ecdysone controls all the moults throughout development,
382 *drs* expression increases in response to this hormone specifically at pupariation, when Br is
383 expressed in Holometabola (25,43). The regulation of AMPs by Br is also fecund regarding
384 the interpretation of AMP expression throughout development between holo- and
385 hemimetabolan insects. Johnston and colleagues demonstrated that these two insect groups
386 have different AMP expression patterns, with holometabolans showing a strong upregulation
387 of immunity that coincides with metamorphosis timing and Br expression(44). In contrast,
388 hemimetabolans do not undergo a dramatic increase in immunity, possibly correlating with
389 much less drastic changes in body remodelling during progressive metamorphosis. In
390 accordance, there is indication that insects with complete metamorphosis suffer a reduction in
391 density, diversity and altered composition of bacterial populations during metamorphosis (45–
392 47), whereas those with incomplete metamorphosis show a constant increase in microbial
393 density and diversity throughout development (48). These data, as ours, are consistent with
394 the previously proposed hypothesis that complete metamorphosis elicits a prophylactic
395 immune response (15,16). However, until now it was unclear how ecdysone could temporally
396 regulate the expression of AMPs at pupariation.
397 Alterations in immunity at life stages with higher risk of infection seem to be a
398 general feature of development, finding some parallels in both vertebrates and invertebrates.
399 In *Drosophila triauraria*, genes of the *drs* family are induced during diapause, which is also
400 considered to be a more susceptible period (49). Most interestingly, data from *Xenopus* also

401 point towards an association between the timing of metamorphosis and a shift in the immune
402 response (50). For example, Major Histocompatibility Complex I (MHC class I) molecules,
403 which bind to peptide fragments derived from pathogens, are first detected at the beginning of
404 metamorphosis (51) and the expression of MHC class II molecules is not triggered if
405 metamorphosis is chemically blocked (52).
406 Together, our data suggest a regulatory mechanism through which ecdysone co-opted
407 the immune system possibly to enhance the success of metamorphic processes. This study
408 reveals a novel association between the endocrine and immune systems in *D. melanogaster*,
409 which act both systemically and locally during metamorphosis. This recruitment of immunity
410 mechanisms by the holometabolan metamorphosis programme presents other interesting
411 features. Three AMPs explain around 95% of the peak observed at the L3 to pupal transition.
412 Interestingly, these three AMPs have been co-opted differently and complementarily to
413 produce, what we interpret as a full-fledged immune prophylactic response despite the
414 absence of solid evidence of an antibacterial role for *drsl2* and *drsl5*. However, this
415 speculation is tempting. *Drsl2*, was recruited to one of the main exposed surface epithelia of
416 larvae, the midgut, that undergoes extensive remodelling at metamorphosis and *drs* is
417 produced in the fat body at metamorphosis initiation, exerting its antibacterial action in a
418 systemic fashion. These two mechanisms, with local and systemic action, share ecdysone
419 control and account for close to 70% of the pupariation AMP peak.
420 This multi-layered developmentally-regulated immune response at the onset of
421 pupariation underscores the sophistication and versatility of the co-option process (53–59)
422 and hints at a possible contribution of this process to the success of metamorphosis as a
423 whole.
424

425 **Materials and methods**

426 *Drosophila* stocks and husbandry

427 If not otherwise noticed, *w[1118]* flies were obtained from Dr. Luís Teixeira
428 (Instituto Gulbenkian de Ciência, Portugal) and used as the reference wild-type strain. The
429 following lines were obtained from the Bloomington Drosophila Stock Center: *w;UAS-*
430 *mCD8GFP* (#5137), *Cg-Gal4* (#7011), *tub-Gal80[ts]*(#7017), *w; UAS-Cas9 P2*(#58986),
431 *w;UAS-brZ4* (#51193) and *w;UAS-dsBroad* (#104648). Several stocks were generously
432 shared by our colleagues, Drs Lynn Riddiford, University of Washington, USA (*w;UAS-*

433 *EcRADN TP3 W650A*), Marc Dionne, Imperial College London, UK (*Hml-Gal4*), François
434 Leulier, IGFL, France (*Mex-Gal4*), Kim Rewitz, University of Copenhagen, Denmark (*AkhR-*
435 *Gal4*), Bruno Lemaitre, EPFL, Switzerland (*iso;iso;Drs*$^{r(w+)}$ and the respective background
436 control). The rescue lines *w;UAS-mCD8GFP; P{UAS-br.Z4}37-6* and *w;UAS-EcRADN TP3*
437 *W650A; P{UAS-br.Z4}37-6* were generated in house at Instituto Gulbenkian de Ciência
438 (Portugal) by the Fly Transgenesis Service (Dr Gastón Guilgur). Standardly raised flies were
439 kept on food with the following composition (g/mL): 4,5% molasse, 7,5% sugar, 7%
440 cornmeal, 2% yeast extract, 1% agar, 2,5% Nipagin 10%. All fly lines we kept at 25ºC in a
441 12L:12D photoperiod. For the ecdysone decreased sensitivity experiment and tissue specific
442 CRISPR, animals were maintained at 17ºC until the moult to the L3 and then transferred to
443 29ºC to activate Gal4 activity.

444 <u>CRISPR knock-out flies</u>

445 The tissue-specific UAS *br* CRISPR knockout constructs were cloned into pCFD6
446 vector (www.crisprflydesign.org, Addgene #73915) according to manufacturer's instructions.
447 Four independent gRNA constructs were cloned to target introns (see primers listed in S9
448 Table) of the *br* core region genomic DNA sequence for *br* common construct and Z4 isoform
449 specific sequence for *br-Z4* construct to target only native genes but not transgenes. After
450 sequenced, the constructs were inserted on either the second chromosome in a recipient line
451 carrying phiC31 integrase and attP40 landing cite with an in-house modified line (*y,w,*
452 *P{y+.nos-int.NLS}; P{CaryP y+}attP40*) or the third chromosome in a recipient line carrying
453 phiC31 integrase and attP2 landing site, *y,w, P(y[+].nos-int. NLS); P(CaryP)attP2* (gift from
454 Dr. Diogo Manoel, Sidra Medical and Research Center, Qatar). Transgenesis was carried out
455 in-house at Instituto Gulbenkian de Ciência (Portugal) by the Fly Transgenesis Service (Dr
456 Gastón Guilgur).

457 <u>Larval and pupal staging</u>

458 Larvae were resynchronized every 2h and kept in normal food for the appropriate
459 time before collection in Trizol. Egg collections were performed on standard *Drosophila* food
460 plates at 25ºC, unless mentioned otherwise. All larvae used for this study were resynchronised
461 either at the onset of the L2 or L3, as previously described (60). Eggs were collected every 4
462 hours and larval densities kept around 200 larvae/60 mm diameter plate. Newly moulted L2
463 or L3 larvae were collected every 2 hours. Collected larvae (up to a maximum of 30
464 larvae/vial) were raised in vials with standard food at 25°C for an additional twenty-four
465 hours. Staged larvae were collected in Trizol for RNA extraction and stored at -80ºC until

466 use. For collection of white pre-pupae (P0), bottles with L3 larvae were monitored every 20
467 minutes, between 48 and 72h after the moult to the L3. Across this study, P0 were identified
468 as motionless pre-pupae with evaginated anterior spiracles. After collection, samples were
469 immediately stored in Trizol and stored at -80ºC until RNA extraction.

470 P0 and pharate adult collection and plating

471 P0 samples were collected as aforementioned. Pharate adults were identified as fully
472 developed adults (with tanned wings and pigmented eyes) still to eclose. Pharate adults were
473 dissected out of the pupal case and collected in 20 minutes intervals 48h to 72h after P0
474 collection. All samples were surface sterilized once with Milli-Q water, 70% ethanol and 13%
475 bleach and rinsed (3x) with sterile water to eliminate bleach traces. After these treatments,
476 each pupa was macerated in 300 µL of LB medium, of which 50 µL were spread onto MRS or
477 D-Mannitol plates. The plates were incubated at 25ºC for 48h for bacterial growth. For each
478 stage and medium a sample size of 100 pupae/pharate was collected per genotype.

479 Statistical analysis for bacterial growth across stages

480 To compare the pattern of variation between P0 and pharate adults across genotypes,
481 we followed a resampling strategy (61): the initial sample was resampled in subsets of 50
482 entries, with no replacement, 2000 times, generating a simulated dataset. In each cycle, a
483 negative binomial regression (*glm.nb(datat$cfu_pupae ~ data$Stage)*) – which does not
484 assume the variance and the mean of the data to be equivalent - was performed to model the
485 change of bacteria according to the stage, generating a regression coefficient, or slope.
486 At the end of the 2000th cycle, a set of these coefficients was obtained for each
487 genotype. This strategy allows us to estimate a set of values that the negative binomial
488 generalized linear regressions may assume, instead of getting just one value. In turn, this set
489 can allow us to explore location and variation statistics, as well as better estimate the
490 parameters of the sampling distribution of the coefficients, with a better notion of its
491 precision.
492 Subsequently, we assessed if the central tendency of the population is greater or less
493 than 0 using one-sided hypothesis tests. In parallel, a measure of the effect size was also
494 calculated. Following a Shapiro-Wilk test of normality, a parametric or non-parametric
495 approach for hypothesis testing and effect size calculation was applied. All data was analysed
496 and all graphics were generated using Rstudio 1.2.5033.

497 Germ-free flies

498 Newly laid eggs were collected into a sterile embryo basket and washed with
499 autoclaved MilliQ water. The eggs were dechorionated and sterilised using a 13% Bleach
500 solution (Sigma Aldrich®) for 10 minutes, washed again with Milli-Q water and sterilized
501 using a 1% Virkon solution for 2 minutes. The sterilized embryos were transferred to axenic
502 media with or without antibiotics (200 mg/mL Rifampicin, 100 mg/mL Tetracycline, 100
503 mg/mL Streptomycin, 15 mg/mL gentamicin). The axenic media contained all the normal
504 ingredients of fly food, is autoclaved prior to use and supplemented with the fungicide
505 Bavistin, which guarantees absence of any traces of microorganisms, including yeast. All
506 plates and bottles were kept inside sterilised containers at 25ºC and all manipulations were
507 conducted in a horizontal flood hood, using sterile materials. After the treatment, the germ-
508 free status was validated by plating surface-sterilized adult flies (from both germ free and
509 control conditions) onto MRS and D- Mannitol media.

510 RNA extraction, cDNA synthesis and real-quantitative PCR

511 RNA was isolated using the Direct-zol™ RNA MiniPrep Kit (Zymo®), following
512 manufacturer's instructions. DNase I treatment and cDNA synthesis were preformed using
513 the RQ1 RNASE-FREE DNASE 1* (Promega®) and the RevertAid H Minus First
514 Strand cDNA Synthesis Kit (Thermo Scientific®), respectively. qPCR was performed using
515 the SYBR® Green PCR Master Mix (Applied Biosystems®) and ABI 7900HT (Applied
516 Biosystems). The PCR conditions used in all experiments were: initial denaturation/ enzyme
517 activation, 95ºC for 10'; followed by 45 cycles of denaturation, 95ºC for 10"; annealing, 60ºC
518 for 10"; extension, 72ºC for 30". Specificity of PCR amplification was verified by melting
519 curve: 95ºC for 10", 65ºC for 1', 97ºC for 1"; cooling, 37ºC, 30". Primers used for all qPCR
520 reactions are represented in S10 Table. Foldchange was determined using the ΔΔCT method,
521 which compares the expression of a given gene of interest to a housekeeping gene between
522 experimental and control samples (62,63). Control L3 samples were used as reference. The
523 data was analysed with a general linear model, using the genotype, stage and gene as
524 explicable variables, as follows: glm(log(Foldchange)~Genotype*Stage*Gene, data=mydata).
525 The expression level for each gene at P0 and pharate was compared within and between
526 genotypes through multiple comparisons using the *lsmeans* package from Rstudio 1.2.5033.

527 Br binding sites prediction

528 The DNA binding motif matrix for Br-Z4 was obtained from the JASPAR database
529 (http://jaspar.genereg.net) and the 5' 2kb region of the *drosomycin* gene was acquired in

Flybase (http://flybase.org). Both sequences were uploaded in FIMO software (http://meme-suite.org/tools/fimo) (33), using a p-value < 0.0001 as a filter.

Acknowledgements

We thank Drs Lynn Riddiford, Marc Dionne, Luís Teixeira, Bruno Lemaitre, François Leulier, Kim Rewitz and Pedro Domingos for stock sharing. We thank Liliana Vieira and Sandra Crisóstomo for technical assistance, Gastón Guilgur for transgenesis services and André Barros for help with statistical analysis. Stocks obtained from the Bloomington Drosophila Stock Center (NIH P40OD018537) were used in this study. This work was supported by: Instituto Gulbenkian de Ciência/Fundação Calouste Gulbenkian; Fundação para a Ciência e a Tecnologia (FCT, Portugal) to CN (PD/BD/114344/2016); CONGENTO, project LISBOA-01-0145-FEDER-022170, co-financed by Lisboa Regional Operational Programme (Lisboa 2020), under the Portugal 2020 Partnership Agreement, through the European Regional Development Fund (ERDF), and Fundação para a Ciência e a Tecnologia (FCT, Portugal).

Author Contributions

CN, Conceptualization, Formal analysis, Investigation, Visualization, Methodology, Writing—original draft, review and editing;
TK, Conceptualization, Investigation, Methodology, Writing—review and editing;
ES, Conceptualization, Supervision, Investigation, Funding acquisition, Methodology, Writing—original draft, review and editing.

549 # References

550 1. Nijhout HF. Insect hormones. Princept: Princeton University Press; 1994.
551 2. Gilbert, L. I., Rybczynski, R., Tobe SS. Endocrine cascade in insect metamorphosis. In: Gilbert,
552 L.I., Tata, J.R., Atkinson BG, editor. Metamorphosis, postembryonic reprogramming of gene
553 expression in amphibian and insect cells. Academic Press Inc; 1996. p. 59–107.
554 3. Webster JI, Tonelli L, Sternberg EM. Neuroendocrine regulation of immunity. Annu Rev Immunol.
555 2002;20(1):125–63.
556 4. Rus F, Flatt T, Tong M, Aggarwal K, Okuda K, Kleino A, et al. Ecdysone triggered PGRP-LC
557 expression controls Drosophila innate immunity. EMBO J [Internet]. 2013;32(11):1626–38.
558 Available from: http://dx.doi.org/10.1038/emboj.2013.100
559 5. Flatt T, Heyland A, Rus F, Porpiglia E, Sherlock C, Yamamoto R, et al. Hormonal regulation of the
560 humoral innate immune response in Drosophila melanogaster. J Exp Biol. 2008;211(16):2712–24.
561 6. Regan JC, Brandão AS, Leitão AB, Mantas Dias ÂR, Sucena É, Jacinto A, et al. Steroid hormone
562 signaling is essential to regulate innate immune cells and fight bacterial infection in Drosophila.
563 PLoS Pathog. 2013;9(10).
564 7. Dimarcq JL, Imler JL, Lanot R, Ezekowitz RAB, Hoffmann JA, Janeway CA, et al. Treatment of
565 l(2)mbn Drosophila tumorous blood cells with the steroid hormone ecdysone amplifies the
566 inducibility of antimicrobial peptide gene expression. Insect Biochem Mol Biol. 1997;27(10):877–
567 86.
568 8. Wang JL, Chen L, Tang L, Zhao HB, Liu XS, Wang YF. 20-hydroxyecdysone transcriptionally
569 regulates humoral immunity in the fat body of Helicoverpa armigera. Insect Mol Biol.
570 2014;23(6):842–56.
571 9. Nunes C, Sucena É, Koyama T. Endocrine regulation of immunity in insects. FEBS J. 2020;(2):1–
572 20.
573 10. Hoffmann JA, Reichhart JM, Hetru C. Innate immunity in higher insects. Curr Opin Immunol.
574 1996;8(1):8–13.
575 11. Du Pasquier L. The immune system of invertebrates and vertebrates. Comp Biochem Physiol - B
576 Biochem Mol Biol. 2001;129(1):1–15.
577 12. Lemaitre B, Hoffmann J. The host defense of Drosophila melanogaster. Annu Rev Immunol.
578 2007;25(1):697–743.
579 13. Cociancich S, Bulet P, Hetru C, Hoffmann JA. The inducible antibacterial peptides of insects.
580 Parasitol Today. 1994;10(4):132–9.
581 14. Yu XQ, Kanost MR. Developmental expression of Manduca sexta hemolin. Arch Insect Biochem
582 Physiol. 1999;42(3):198–212.
583 15. Russell VW, Dunn PE. Lysozyme in the midgut of Manduca sexta during metamorphosis.
584 1991;80(12777):67–80.
585 16. Russell V, Dunn PE. Antibacterial proteins in the midgut of Manduca sexta during metamorphosis. J
586 Insect Physiol. 1996;42(1):65–71.
587 17. Hakim RS, Baldwin K, Smagghe G. Regulation of midgut growth, development, and

588 metamorphosis. Annu Rev Entomol. 2010;55(1):593–608.
589 18. Judy KJ, Gilbert LI. Histology of the alimentary canal during the metamorphosis of Hyalophora
590 cecropia (L.). J Morphol. 1970;131(3):277–99.
591 19. Bacot A. On the persistence of Bacilli in the gut of an Insect during metamorphosis. Parasitology.
592 1911;4:497–500.
593 20. Leach JG. The method of survival of bacteria in the puparia of the seed-corn maggot (Hylemyia
594 Cilicrura Rond.). Zeitschrift für Angew Entomol. 1934;20(1):150–61.
595 21. Bakula M. The persistence of a microbial flora during postembryogenesis of Drosophila
596 melanogaster. J Invertebr Pathol. 1969;14(3):365–74.
597 22. Duneau DF, Lazzaro BP. Persistence of an extracellular systemic infection across metamorphosis in
598 a holometabolous insect. Biol Lett. 2018;14(2):10–3.
599 23. Thurmond J, Goodman JL, Strelets VB, Attrill H, Gramates LS, Marygold SJ, et al. FlyBase 2.0:
600 The next generation. Nucleic Acids Res. 2019;47(D1):D759–65.
601 24. Zhang Z, Palli SR. Identification of a cis-regulatory element required for 20-hydroxyecdysone
602 enhancement of antimicrobial peptide gene expression in Drosophila melanogaster. Insect Mol Biol.
603 2009;18(5):595–605.
604 25. Zhou X, Riddiford LM. Broad specifies pupal development and mediates the "status quo" action of
605 juvenile hormone on the pupal-adult transformation in Drosophila and Manduca. Development.
606 2002;129(9):2259–69.
607 26. Cherbas L, Hu X, Zhimulev I, Belyaeva E, Cherbas P. EcR isoforms in Drosophila: Testing tissue-
608 specific requirements by targeted blockade and rescue. Development. 2003;130(2):271–84.
609 27. Davis MM, Engström Y. Immune response in the barrier epithelia: Lessons from the fruit fly
610 Drosophila melanogaster. J Innate Immun. 2012;4(3):273–83.
611 28. Truman JW, Riddiford LM. The origins of insect metamorphosis. Nature [Internet]. 1999 Sep
612 30;401(6752):447–52. Available from: http://dx.doi.org/10.1038/46737
613 29. Belles X. Origin and evolution of insect metamorphosis. eLS. 2011;1–11.
614 30. Port F, Chen HM, Lee T, Bullock SL. Optimized CRISPR/Cas tools for efficient germline and
615 somatic genome engineering in Drosophila. Proc Natl Acad Sci U S A. 2014;111(29).
616 31. Xue Z, Wu M, Wen K, Ren M, Long L, Zhang X, et al. CRISPR/Cas9 mediates efficient conditional
617 mutagenesis in Drosophila. G3 Genes, Genomes, Genet. 2014;4(11):2167–73.
618 32. Mai T, Chen S, Lin X, Zhang X, Zou X, Feng Q, et al. 20-hydroxyecdysone positively regulates the
619 transcription of the antimicrobial peptide, lebocin, via BmEts and BmBR-C Z4 in the midgut of
620 Bombyx mori during metamorphosis. Dev Comp Immunol [Internet]. 2017;74:10–8. Available
621 from: http://dx.doi.org/10.1016/j.dci.2017.04.002
622 33. Grant CE, Bailey TL, Noble WS. FIMO: Scanning for occurrences of a given motif. Bioinformatics.
623 2011;27(7):1017–8.
624 34. Buchon N, Broderick NA, Poidevin M, Pradervand S, Lemaitre B. Drosophila Intestinal Response
625 to Bacterial Infection: Activation of Host Defense and Stem Cell Proliferation. Cell Host Microbe
626 [Internet]. 2009;5(2):200–11. Available from: http://dx.doi.org/10.1016/j.chom.2009.01.003
627 35. Lemaitre B, Reichhart JM, Hoffmann JA. Drosophila host defense: Differential induction of

628 antimicrobial peptide genes after infection by various classes of microorganisms. Proc Natl Acad
629 Sci U S A. 1997;94(26):14614–9.
630 36. Leulier F, Rodriguez A, Khush RS, Abrams JM, Lemaitre B. The Drosophila caspase Dredd is
631 required to resist Gram-negative bacterial infection. EMBO Rep. 2000;1(4):353–8.
632 37. Foley E, O'Farrell PH. Nitric oxide contributes to induction of innate immune responses to gram-
633 negative bacteria in Drosophila. Genes Dev. 2003;17(1):115–25.
634 38. Tanji T, Hu X, Weber ANR, Ip YT. Toll and IMD pathways synergistically activate an innate
635 Immune Response in Drosophila melanogaster. Mol Cell Biol. 2007;27(12):4578–88.
636 39. Li Y, Li S, Li R, Xu J, Jin P, Chen L, et al. Genome-wide miRNA screening reveals miR-310 family
637 members negatively regulate the immune response in Drosophila melanogaster via co-targeting
638 Drosomycin. Dev Comp Immunol [Internet]. 2017;68:34–45. Available from:
639 http://dx.doi.org/10.1016/j.dci.2016.11.014
640 40. Zhan MY, Yang PJ, Rao XJ. Molecular cloning and analysis of PGRP-L1 and IMD from silkworm
641 Bombyx mori [Internet]. Vol. 215, Comparative Biochemistry and Physiology Part - B:
642 Biochemistry and Molecular Biology. Elsevier Inc; 2018. 19–30 p. Available from:
643 http://dx.doi.org/10.1016/j.cbpb.2017.10.002
644 41. Tzou P, Ohresser S, Ferrandon D, Capovilla M, Reichhart J, Lemaitre B, et al. Tissue-specific
645 inducible expression of antimicrobial peptide genes in Drosophila surface epithelia. 2000;13:737–
646 48.
647 42. Ma H, Abbas MN, Zhang K, Hu X, Xu M, Liang H, et al. 20-Hydroxyecdysone regulates the
648 transcription of the lysozyme via Broad-Complex Z2 gene in silkworm, Bombyx mori. Dev Comp
649 Immunol [Internet]. 2019;94(November 2018):66–72. Available from:
650 https://doi.org/10.1016/j.dci.2019.01.014
651 43. Erezyilmaz DF, Riddiford LM, Truman JW. The pupal specifier broad directs progressive
652 morphogenesis in a direct-developing insect. Proc Natl Acad Sci U S A. 2006;103(18):6925–30.
653 44. Johnston PR, Paris V ronique, Rolff J. Immune gene regulation in the gut during metamorphosis in a
654 holo- versus a hemimetabolous insect. Philos Trans R Soc B Biol Sci. 2019;374(1783):1–6.
655 45. Johnston PR, Rolff J. Host and Symbiont Jointly Control Gut Microbiota during Complete
656 Metamorphosis. PLoS Pathog. 2015;11(11):1–11.
657 46. Hammer TJ, McMillan WO, Fierer N. Metamorphosis of a butterfly-associated bacterial
658 community. PLoS One. 2014;9(1).
659 47. Kim JK, Han SH, Kim CH, Jo YH, Futahashi R, Kikuchi Y, et al. Molting-associated suppression of
660 symbiont population and up-regulation of antimicrobial activity in the midgut symbiotic organ of
661 the Riptortus-Burkholderia symbiosis. Dev Comp Immunol [Internet]. 2014;43(1):10–4. Available
662 from: http://dx.doi.org/10.1016/j.dci.2013.10.010
663 48. Sudakaran S, Salem H, Kost C, Kaltenpoth M. Geographical and ecological stability of the
664 symbiotic mid-gut microbiota in European firebugs, Pyrrhocoris apterus (Hemiptera,
665 Pyrrhocoridae). Mol Ecol. 2012;21(24):6134–51.
666 49. Daibo S, Kimura MT, Goto SG. Upregulation of genes belonging to the drosomycin family in
667 diapausing adults of Drosophila triauraria. Gene. 2001;278(1–2):177–84.

668 50. Robert J, Ohta Y. Comparative and developmental study of the immune system in Xenopus. Dev
669 Dyn. 2009;238(6):1249–70.
670 51. Flajnik MF, Du Pasquier L. MHC class I antigens as surface markers of adult erythrocytes during
671 the metamorphosis of Xenopus. Dev Biol. 1988;128(1):198–206.
672 52. Rollins-Smith LA, Blair P. Expression of class II major histocompatibility complex antigens on
673 adult T cells in Xenopus is metamorphosis-dependent. Dev Immunol. 1990;1:97–104.
674 53. McQueen E, Rebeiz M. On the specificity of gene regulatory networks: How does network co-
675 option affect subsequent evolution? [Internet]. 1st ed. Vol. 139, Current Topics in Developmental
676 Biology. Elsevier Inc.; 2020. 375–405 p. Available from:
677 http://dx.doi.org/10.1016/bs.ctdb.2020.03.002
678 54. Denise R, Abby SS, Rocha EPC. The Evolution of Protein Secretion Systems by Co-option and
679 Tinkering of Cellular Machineries. Trends Microbiol [Internet]. 2020;28(5):372–86. Available from:
680 https://doi.org/10.1016/j.tim.2020.01.005
681 55. Duncan EJ, Johnson TK, Whisstock JC, Warr CG DP. Capturing embryonic development from
682 metamorphosis: how did the terminal patterning signalling pathway of Drosophila evolve? Curr
683 Opin Insect Sci. 2014;(1):45–51.
684 56. Vreede BMI, Lynch JA, Roth S, Sucena É. Co-option of a coordinate system defined by the EGFr
685 and Dpp pathways in the evolution of a morphological novelty. Evodevo. 2013;4(1):1–12.
686 57. Litman GW, Rast JP, Fugmann SD. The origins of vertebrate adaptive immunity. Nat Rev Immunol.
687 2010;10(8):543–53.
688 58. Peel AD. The evolution of developmental gene networks: Lessons from comparative studies on
689 holometabolous insects. Philos Trans R Soc B Biol Sci. 2008;363(1496):1539–47.
690 59. True JR, Carroll SB. Gene co-option in physiological and morphological evolution. Annu Rev Cell
691 Dev Biol. 2002;18:53–80.
692 60. Koyama T, Mirth CK. Growth-Blocking Peptides As Nutrition-Sensitive Signals for Insulin
693 Secretion and Body Size Regulation. PLoS Biol. 2016;14(2):1–23.
694 61. Fieberg JR, Vitense K, Johnson DH. Resampling-based methods for biologists. PeerJ. 2020;2020(3).
695 62. Livak KJ, Schmittgen TD. Analysis of relative gene expression data using real-time quantitative
696 PCR and the 2-ΔΔCT method. Methods. 2001;25(4):402–8.
697 63. Schmittgen TD, Livak KJ. Analyzing real-time PCR data by the comparative CT method. Nat
698 Protoc. 2008;3(6):1101–8.
699

Supplementary Figures and Tables

Supplementary Figures

Supplementary Figure 1

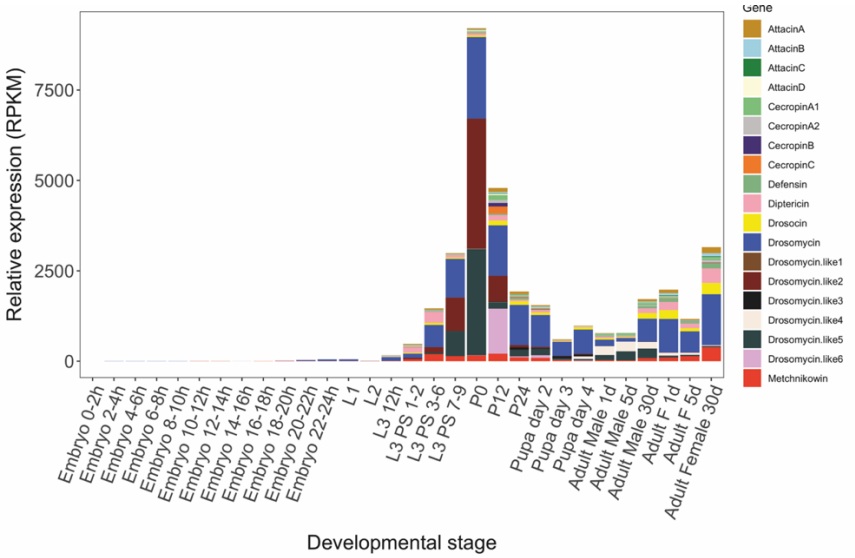

Supplementary Figure 1. High-throughput temporal AMP expression. Expression refers to whole body, with levels represented as linear and scaled to maximum expression (publicly available on Flybase http://flybase.org/ (Thurmond et al., 2019)).

Supplementary Figure 2

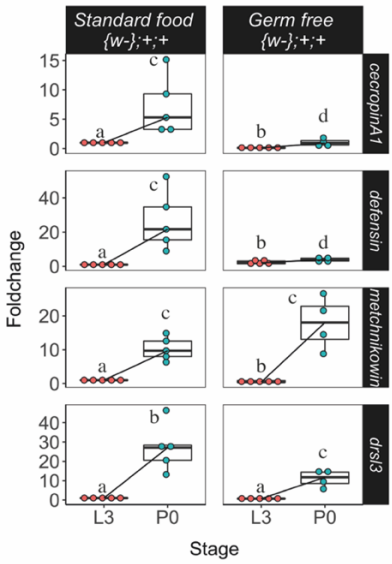

Supplementary Figure 2. The expression levels of *cecropin A1*, *defensin*, *metchnikowin* and *drsl3* increase at pupariation and are not lost in GF conditions, albeit to different degrees.

Supplementary Figure 3

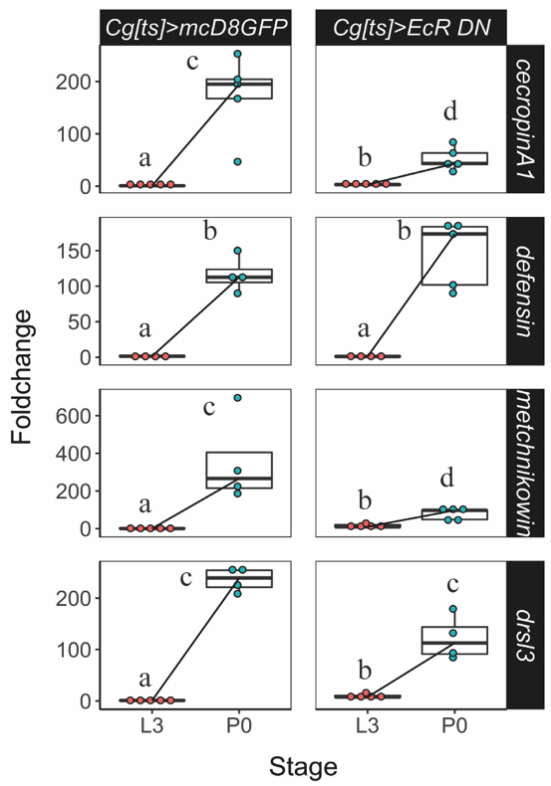

Supplementary Figure 3-1. Reduced expression of ecdysone sensitivity in the fat body and haemocytes does not affect the expression of *cecropin A1*, *defensin*, *metchnikowin* and *drsl3*.

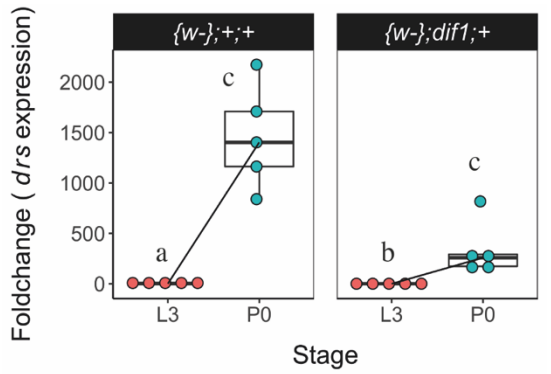

Supplementary Figure 3-2. *drs* expression increases at P0 in *{w-};dif1;+* mutant.

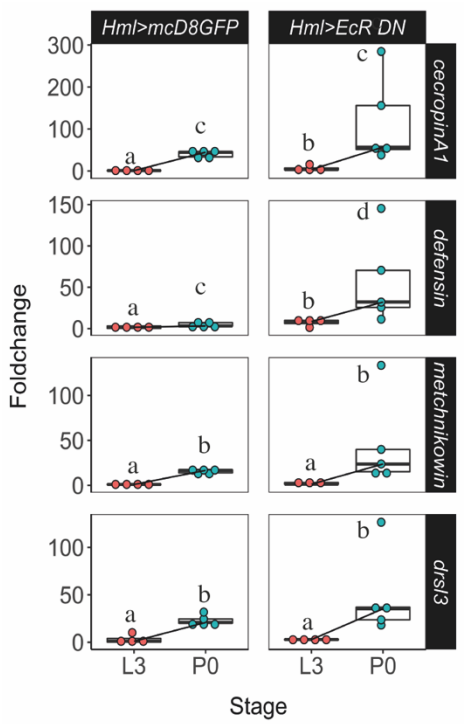

Supplementary Figure 3-3. Reduced ecdysone sensitivity in the haemocytes does not affect the expression of of *cecropin A1*, *defensin*, *metchnikowin* and *drsl3*.

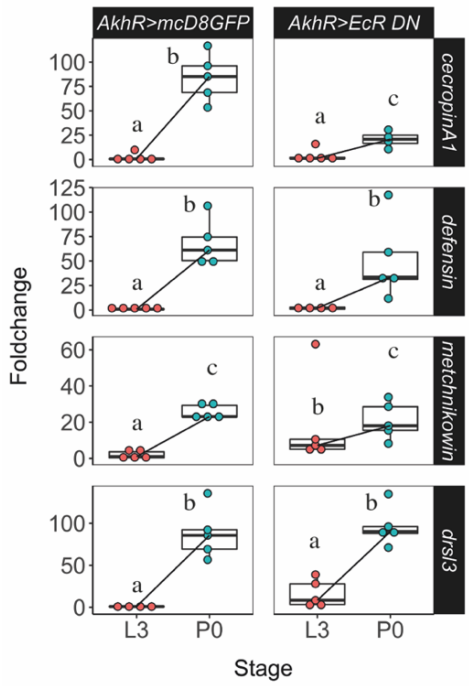

Supplementary Figure 3-4. The expression of *cecropin A1*, *defensin*, *metchnikowin* and *drsl3* is unaffected by decreased ecdysone sensitivity specifically in the fat body.

Supplementary Figure 4

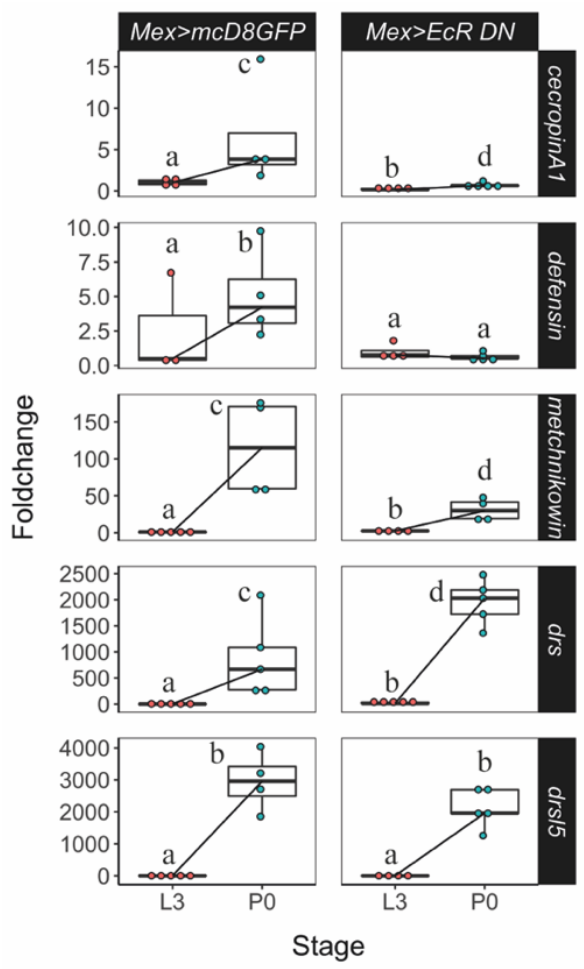

Supplementary Figure 4. Decreased ecdysone signalling in the midgut results in significant decrease in mRNA levels for: *cecropin A1* (*lsmeans(pairwise~Genotype|P0)<0.0001; lsmeans(pairwise~Stage|Mex>EcRDN)= 0.0038), defensin (lsmeans(pairwise~Genotype|P0) <0.0001; lsmeans(pairwise~Stage|Mex>EcRDN)=0.3866*), *metchnikowin* (*lsmeans (pairwise~Genotype|P0)=0.0060; lsmeans (pairwise~Stage|Mex>EcRDN<0.0001*), and *drsl3 ((lsmeans(pairwise~Genotype|P0)=0.0008; lsmeans(pairwise~Stage|Mex>EcRDN)=0.2084*).

Supplementary Figure 5

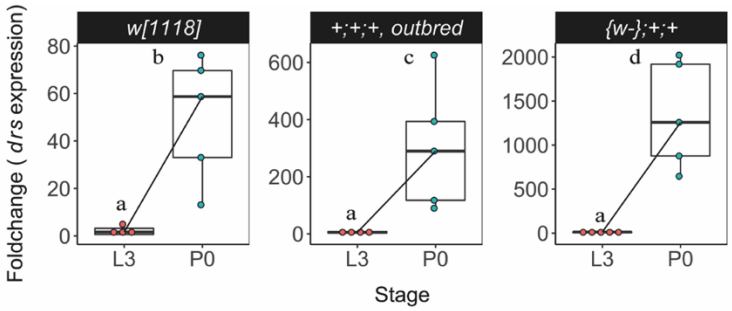

Supplementary Figure 5-1. The expression of *drs* increased at pupariation regardless of the genetic background (*lsmeans(pairwise~Stage|w1118)<0.0001; lsmeans(pairwise~Stage|outbred <0.0001; lsmeans(pairwise~Stage|Iso)<0.0001*). Each dot represents a sample of five pooled individuals; the lines connect the median of the samples at L3 and P0; different letters represent statistically significant differences in fold-change. Fold-change was determined using the ΔΔCT method.

Supplementary Figure 5-2. JASPAR DNA binding motif MA0013.1 for Br-Z4

Motif ID	Alt ID	Sequence Name	Strand	Start	End	p-value	q-value	Matched Sequence
MA0013.1	br(var.4)	Drs	+	1022	1032	8.65e-06	0.0254	AAGTAAACAAA
MA0013.1	br(var.4)	Drs	-	1189	1199	1.9e-05	0.0279	TAATAAACAAC
MA0013.1	br(var.4)	Drs	+	755	765	7.17e-05	0.0703	TAGAAAAGAAA

Supplementary Figure 5-3. Br-Z4 binding motifs predicted by FIMO [29] software (http://meme-suite.org/tools/fimo) to be present in 2kb region of the 5'-end of the *drs* gene, using a p-value<0.0001 as filter.

Supplementary Figure 6

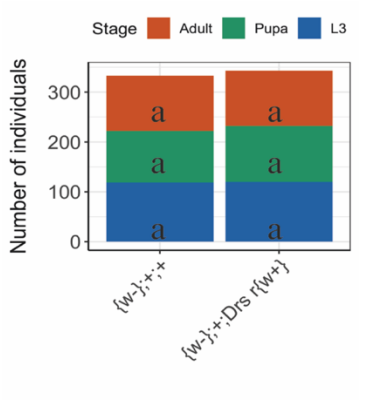

Supplementary Figure 6. Control ({*w-*};+;+) and *drs* mutant ({*w-*};+; *Drs r*{*w+*}) lines showed no differences in mortality between L3, pupae and adults (*lsmeans(pairwise~Stage|Genotype) <0.0001; lsmeans(pairwise~Genotype|Stage)<0.0001*).

Supplementary Figure 7

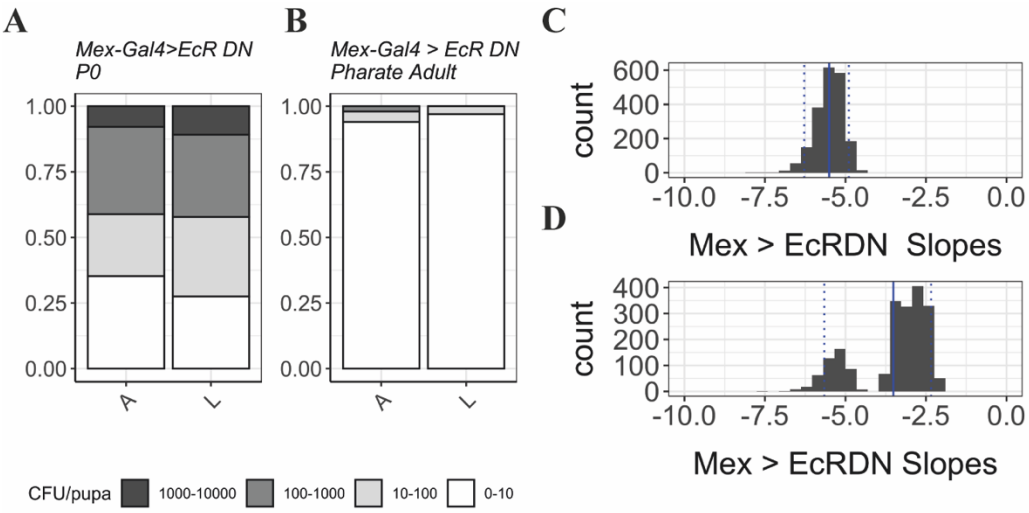

Supplementary Figure 7. (A-B) Quantification in P0 pupae and pharate adults of *Lactobacillus* (L), growing in selective MRS medium, and *Acetobacter* (A), growing on selective D-Mannitol. The number of individuals with more bacteria is greater in P0 samples (A) than in pharate adults (B). Y-axis represents the proportion of individuals in each bacterial count category. (C-D) Coefficient (slopes) distribution in *Mex>EcRDN* samples of *Lactobacillus* (C) (*Median: -5.455 (IQR: -6.279; -4.895); One-way Wilcoxon test for median<0: <2.2e-16, r=0.866*) and *Acetobacter* (D) (*Median: -3.134 (IQR: -5.656; -2.342); One-way Wilcoxon test for median>0: <2.2e-16, r=0.866)*. Doted lines represent the 0.05 and 0.95 quantiles; full line represents the mean slope.

Supplementary Tables

Gene	***lsmeans, pairwise~Genotype | Stage***	***p-value***
cecropin A1	*{w-};+;+* vs *{w-};+;+* GF | L3	<0.0001
	{w-};+;+ vs *{w-};+;+* GF | P0	<0.0001
defensin	*{w-};+;+* vs *{w-};+;+* GF | L3	0.0096
	{w-};+;+ vs *{w-};+;+* GF | P0	<0.0001
metchnikowin	*{w-};+;+* vs *{w-};+;+* GF | L3	0.0089
	{w-};+;+ vs *{w-};+;+* GF | P0	0.1038
drs	*{w-};+;+* vs *{w-};+;+* GF | L3	<0.0001
	{w-};+;+ vs *{w-};+;+* GF | P0	0.0978
drsl2	*{w-};+;+* vs *{w-};+;+* GF | L3	<0.0001
	{w-};+;+ vs *{w-};+;+* GF | P0	0.0226
drsl3	*{w-};+;+* vs *{w-};+;+* GF | L3	0.2113
	{w-};+;+ vs *{w-};+;+* GF | P0	0.0058
drsl5	*{w-};+;+* vs *{w-};+;+* GF | L3	<0.0001
	{w-};+;+ vs *{w-};+;+* GF | P0	0.0105
Gene	***lsmeans, pairwise~Stage | Genotype***	***p-value***
cecropin A1	*{w-};+;+*	<0.0001
	{w-};+;+ GF	<0.0001
defensin	*{w-};+;+*	<0.0001
	{w-};+;+ GF	0.0752
metchnikowin	*{w-};+;+*	<0.0001
	{w-};+;+ GF	<0.0001
drs	*{w-};+;+*	<0.0001
	{w-};+;+ GF	<0.0001
drsl2	*{w-};+;+*	<0.0001
	{w-};+;+ GF	<0.0001
drsl3	*{w-};+;+*	<0.0001
	{w-};+;+ GF	<0.0001
drsl5	*{w-};+;+*	<0.0001
	{w-};+;+ GF	<0.0001

S1 Table. **Statistical analysis of AMPs expression in an isogenic line (*{w-};+;+*) in normal and germ-free (GF) conditions at L3 and P0 stages**. lsmeans, pairwise~Genotype | Stage represents differences within the same stage, between genotypes. lsmeans, pairwise~Stage | Genoype represents the difference between L3 and P0 within each genotype.

Gene	lsmeans, pairwise~Genotype | Stage	p-value
cecropin A1	*Cg[ts]>mcD8GFP* vs *Cg[ts]>EcR DN* | L3	0.0057
	Cg[ts]>mcD8GFP vs *Cg[ts]>EcR DN* | P0	0.0064
defensin	*Cg[ts]>mcD8GFP* vs *Cg[ts]>EcR DN* | L3	0.8361
	Cg[ts]>mcD8GFP vs *Cg[ts]>EcR DN* | P0	0.6428
metchnikowin	*Cg[ts]>mcD8GFP* vs *Cg[ts]>EcR DN* | L3	<0.0001
	Cg[ts]>mcD8GFP vs *Cg[ts]>EcR DN* | P0	0.0012
drs	*Cg[ts]>mcD8GFP* vs *Cg[ts]>EcR DN* | L3	0.7558
	Cg[ts]>mcD8GFP vs *Cg[ts]>EcR DN* | P0	<0.0001
drsl2	*Cg[ts]>mcD8GFP* vs *Cg[ts]>EcR DN* | L3	0.6216
	Cg[ts]>mcD8GFP vs *Cg[ts]>EcR DN* | P0	0.0192
drsl3	*Cg[ts]>mcD8GFP* vs *Cg[ts]>EcR DN* | L3	<0.0001
	Cg[ts]>mcD8GFP vs *Cg[ts]>EcR DN* | P0	0.1326
drsl5	*Cg[ts]>mcD8GFP* vs *Cg[ts]>EcR DN* | L3	<0.0001
	Cg[ts]>mcD8GFP vs *Cg[ts]>EcR DN* | P0	0.4561
Gene	**lsmeans, pairwise~Stage | Genotype**	**p-value**
cecropin A1	*Cg[ts]>mcD8GFP* | L3 vs P0	<0.0001
	Cg[ts]>EcR DN | L3 vs P0	<0.0001
defensin	*Cg[ts]>mcD8GFP* | L3 vs P0	<0.0001
	Cg[ts]>EcR DN | L3 vs P0	<0.0001
metchnikowin	*Cg[ts]>mcD8GFP* | L3 vs P0	<0.0001
	Cg[ts]>EcR DN | L3 vs P0	<0.0001
drs	*Cg[ts]>mcD8GFP* | L3 vs P0	<0.0001
	Cg[ts]>EcR DN | L3 vs P0	0..0017
drsl2	*Cg[ts]>mcD8GFP* | L3 vs P0	<0.0001
	Cg[ts]>EcR DN | L3 vs P0	<0.0001
drsl3	*Cg[ts]>mcD8GFP* | L3 vs P0	<0.0001
	Cg[ts]>EcR DN | L3 vs P0	<0.0001
drsl5	*Cg[ts]>mcD8GFP* | L3 vs P0	<0.0001
	Cg[ts]>EcR DN | L3 vs P0	<0.0001

S2 Table. Statistical analysis of AMP expression in samples with decreased ecdysone sensitivity in the fat body and haemocytes (*Cg>EcRDN*). lsmeans, pairwise~Genotype | Stage represents differences within the same stage, between genotypes. lsmeans, pairwise~Stage | Genotype represents the difference between L3 and P0 within each genotype.

Gene	lsmeans, pairwise~Genotype | Stage	p-value
cecropin A1	*Hml>mcD8GFP* vs *Hml>EcR DN* | L3	0.0047
	Hml>mcD8GFP vs *Hml>EcR DN* | P0	0.1124
defensin	*Hml>mcD8GFP* vs *Hml>EcR DN* | L3	0.0012
	Hml>mcD8GFP vs *Hml>EcR DN* | P0	<0.0001
metchnikowin	*Hml>mcD8GFP* vs *Hml>EcR DN* | L3	0.2988
	Hml>mcD8GFP vs *Hml>EcR DN* | P0	0.1739
drs	*Hml>mcD8GFP* vs *Hml>EcR DN* | L3	0.0033
	Hml>mcD8GFP vs *Hml>EcR DN* | P0	0.0185
drsl2	*Hml>mcD8GFP* vs *Hml>EcR DN* | L3	0.0512
	Hml>mcD8GFP vs *Hml>EcR DN* | P0	0.8840
drsl3	*Hml>mcD8GFP* vs *Hml>EcR DN* | L3	0.0732
	Hml>mcD8GFP vs *Hml>EcR DN* | P0	0.3020
drsl5	*Hml>mcD8GFP* vs *Hml>EcR DN* | L3	0.0065
	Hml>mcD8GFP vs *Hml>EcR DN* | P0	0.1605
Gene	**lsmeans, pairwise~Stage | Genotype**	**p-value**
cecropin A1	*Hml>mcD8GFP* | L3 vs P0	<0.0001
	Hml>EcR DN | L3 vs P0	<0.0001
defensin	*Hml>mcD8GFP* | L3 vs P0	0.0118
	Hml>EcR DN | L3 vs P0	0.0003
metchnikowin	*Hml>mcD8GFP* | L3 vs P0	<0.0001
	Hml>EcR DN | L3 vs P0	<0.0001
drs	*Hml>mcD8GFP* | L3 vs P0	<0.0001
	Hml>EcR DN | L3 vs P0	<0.0001
drsl2	*Hml>mcD8GFP* | L3 vs P0	<0.0001
	Hml>EcR DN | L3 vs P0	<0.0001
drsl3	*Hml>mcD8GFP* | L3 vs P0	<0.0001
	Hml>EcR DN | L3 vs P0	<0.0001
drsl5	*Hml>mcD8GFP* | L3 vs P0	<0.0001
	Hml>EcR DN | L3 vs P0	<0.0001

S3 Table. Statistical analysis of AMP expression in samples with decreased ecdysone sensitivity in haemocytes (*Hml>EcRDN*). lsmeans, pairwise~Genotype | Stage represents differences within the same stage, between genotypes. lsmeans, pairwise~Stage | Genotype represents the difference between L3 and P0 within each genotype.

Gene	lsmeans, pairwise~Genotype | Stage	p-value
cecropin A1	*AkhR>mcD8GFP* vs *AkhR>EcR DN* | L3	0.2413
	AkhR>mcD8GFP vs *AkhR>EcR DN* | P0	0.0228
defensin	*AkhR>mcD8GFP* vs *AkhR>EcR DN* | L3	0.4736
	AkhR>mcD8GFP vs *AkhR>EcR DN* | P0	0.3747
metchnikowin	*AkhR>mcD8GFP* vs *AkhR>EcR DN* | L3	0.0001
	AkhR>mcD8GFP vs *AkhR>EcR DN* | P0	0.5902
drs	*AkhR>mcD8GFP* vs *AkhR>EcR DN* | L3	0.0133
	AkhR>mcD8GFP vs *AkhR>EcR DN* | P0	<0.0001
drsl2	*AkhR>mcD8GFP* vs *AkhR>EcR DN* | L3	0.7280
	AkhR>mcD8GFP vs *AkhR>EcR DN* | P0	0.4609
drsl3	*AkhR>mcD8GFP* vs *AkhR>EcR DN* | L3	0.0001
	AkhR>mcD8GFP vs *AkhR>EcR DN* | P0	0.8518
drsl5	*AkhR>mcD8GFP* vs *AkhR>EcR DN* | L3	0.0058
	AkhR>mcD8GFP vs *AkhR>EcR DN* | P0	0.3890
Gene	**lsmeans, pairwise~Stage | Genotype**	**p-value**
cecropin A1	*AkhR>mcD8GFP* | L3 vs P0	<0.0001
	AkhR>EcR DN | L3 vs P0	0.0003
defensin	*AkhR>mcD8GFP* | L3 vs P0	<0.0001
	AkhR>EcR DN | L3 vs P0	<0.0001
metchnikowin	*AkhR>mcD8GFP* | L3 vs P0	<0.0001
	AkhR>EcR DN | L3 vs P0	0.3266
drs	*AkhR>mcD8GFP* | L3 vs P0	<0.0001
	AkhR>EcR DN | L3 vs P0	0.6709
drsl2	*AkhR>mcD8GFP* | L3 vs P0	<0.0001
	AkhR>EcR DN | L3 vs P0	<0.0001
drsl3	*AkhR>mcD8GFP* | L3 vs P0	<0.0001
	AkhR>EcR DN | L3 vs P0	0.0001
drsl5	*AkhR>mcD8GFP* | L3 vs P0	<0.0001
	AkhR>EcR DN | L3 vs P0	<0.0001

S4 Table. Statistical analysis of AMP expression in samples with decreased ecdysone sensitivity in the fat body (*AkhR>EcRDN*). lsmeans, pairwise~Genotype | Stage represents differences within the same stage, between genotypes. lsmeans, pairwise~Stage | Genotype represents the difference between L3 and P0 within each genotype.

Gene	lsmeans, pairwise~Genotype | Stage	p-value
cecropin A1	*Mex>mcD8GFP* vs *Mex>EcR DN* | L3	0.0004
	Mex>mcD8GFP vs *Mex>EcR DN* | P0	<0.0001
defensin	*Mex>mcD8GFP* vs *Mex>EcR DN* | L3	0.7855
	Mex>mcD8GFP vs *Mex>EcR DN* | P0	<0.0001
metchnikowin	*Mex>mcD8GFP* vs *Mex>EcR DN* | L3	0.0371
	Mex>mcD8GFP vs *Mex>EcR DN* | P0	0.0060
drs	*Mex>mcD8GFP* vs *Mex>EcR DN* | L3	<0.0001
	Mex>mcD8GFP vs *Mex>EcR DN* | P0	0.0076
drsl2	*Mex>mcD8GFP* vs *Mex>EcR DN* | L3	0.8069
	Mex>mcD8GFP vs *Mex>EcR DN* | P0	<0.0001
drsl3	*Mex>mcD8GFP* vs *Mex>EcR DN* | L3	<0.0001
	Mex>mcD8GFP vs *Mex>EcR DN* | P0	0.0008
drsl5	*Mex>mcD8GFP* vs *Mex>EcR DN* | L3	0.9832
	Mex>mcD8GFP vs *Mex>EcR DN* | P0	0.4479
Gene	**lsmeans, pairwise~Stage | Genotype**	**p-value**
cecropin A1	*Mex>mcD8GFP* | L3 vs P0	0.0010
	Mex>EcR DN | L3 vs P0	0.0038
defensin	*Mex>mcD8GFP* | L3 vs P0	0.0028
	Mex>EcR DN | L3 vs P0	0.3866
metchnikowin	*Mex>mcD8GFP* | L3 vs P0	<0.0001
	Mex>EcR DN | L3 vs P0	<0.0001
drs	*Mex>mcD8GFP* | L3 vs P0	<0.0001
	Mex>EcR DN | L3 vs P0	<0.0001
drsl2	*Mex>mcD8GFP* | L3 vs P0	<0.0001
	Mex>EcR DN | L3 vs P0	<0.0001
drsl3	*Mex>mcD8GFP* | L3 vs P0	<0.0001
	Mex>EcR DN | L3 vs P0	0.2084
drsl5	*Mex>mcD8GFP* | L3 vs P0	<0.0001
	Mex>EcR DN | L3 vs P0	<0.0001

S5 Table. Statistical analysis of AMP expression in samples with decreased ecdysone sensitivity in the migut (*Mex>EcRDN*). lsmeans, pairwise~Genotype | Stage represents differences within the same stage, between genotypes. lsmeans, pairwise~Stage | Genotype represents the difference between L3 and P0 within each genotype.

Gene	lsmeans, pairwise~Genotype | Stage	p-value
cecropin A1	*Btl>mcD8GFP* vs *Btl>EcR DN* | L3	0.0197
	Btl>mcD8GFP vs *Btl>EcR DN* | P0	0.8417
defensin	*Btl>mcD8GFP* vs *Btl>EcR DN* | L3	0.1219
	Btl>mcD8GFP vs *Btl>EcR DN* | P0	0.0336
metchnikowin	*Btl>mcD8GFP* vs *Btl>EcR DN* | L3	<0.0001
	Btl>mcD8GFP vs *Btl>EcR DN* | P0	0.6789
drs	*Btl>mcD8GFP* vs *Btl>EcR DN* | L3	0.0098
	Btl>mcD8GFP vs *Btl>EcR DN* | P0	0.1636
drsl2	*Btl>mcD8GFP* vs *Btl>EcR DN* | L3	0.0197
	Btl>mcD8GFP vs *Btl>EcR DN* | P0	0.9116
drsl3	*Btl>mcD8GFP* vs *Btl>EcR DN* | L3	<0.0001
	Btl>mcD8GFP vs *Btl>EcR DN* | P0	0.4955
drsl5	*Btl>mcD8GFP* vs *Btl>EcR DN* | L3	0.4510
	Btl>mcD8GFP vs *Btl>EcR DN* | P0	0.1192
Gene	**lsmeans, pairwise~Stage | Genotype**	**p-value**
cecropin A1	*Btl>mcD8GFP* | L3 vs P0	<0.0001
	Btl>EcR DN | L3 vs P0	0.0001
defensin	*Btl>mcD8GFP* | L3 vs P0	0.0027
	Btl>EcR DN | L3 vs P0	0.0010
metchnikowin	*Btl>mcD8GFP* | L3 vs P0	<0.0001
	Btl>EcR DN | L3 vs P0	0.3711
drs	*Btl>mcD8GFP* | L3 vs P0	<0.0001
	Btl>EcR DN | L3 vs P0	<0.0001
drsl2	*Btl>mcD8GFP* | L3 vs P0	<0.0001
	Btl>EcR DN | L3 vs P0	<0.0001
drsl3	*Btl>mcD8GFP* | L3 vs P0	<0.0001
	Btl>EcR DN | L3 vs P0	0.0004
drsl5	*Btl>mcD8GFP* | L3 vs P0	<0.0001
	Btl>EcR DN | L3 vs P0	<0.0001

S6 Table. Statistical analysis of AMP expression in samples with decreased ecdysone sensitivity in the tracheal system (*btl>EcRDN*). lsmeans, pairwise~Genotype | Stage represents differences within the same stage, between genotypes. lsmeans, pairwise~Stage | Genotype represents the difference between L3 and P0 within each genotype.

lsmeans, pairwise~Genotype | Stage	***p-value***
+;+;+ vs *+;+;Drs{w+}* | L3	0.9211
+;+;+ vs *+;+;Drs{w+}* | Pupa	0.2412
+;+;+ vs *+;+;Drs{w+}* | Adult	0.7340
lsmeans, pairwise~Stage | Genotype	***p-value***
+;+;+ | L3 vs Pupa	0.1774
+;+;+ | L3 vs Adult	0.7390
+;+;+ | Pupa vs Adult	1.0000
+;+;Drs{w+} | L3 vs Pupa	1.0000
+;+;Drs{w+} | L3 vs Adult	1.0000
+;+;Drs{w+} | Pupa vs Adult	1.0000

S7 Table. Statistical analysis of mortality between genotypes, across stages. lsmeans, pairwise~Genotype | Stage represents differences within the same stage, between genotypes. lsmeans, pairwise~Stage | Genotype represents the difference between L3 and P0 within each genotype.

Gene	**lsmeans, pairwise~Genotype | Stage**	**p-value**
cecropin A1	*Cg;Cas9>+;+;+* vs *Cg;Cas9>br KO* | L3	1.0000
	Cg;Cas9>+;+;+ vs *Cg;Cas9>br-Z4 KO* | L3	1.0000
	Cg;Cas9>br KO *Cg;Cas9>br-Z4 KO* | L3	1.0000
	Cg;Cas9>+;+;+ vs *Cg;Cas9>br KO* | P0	1.0000
	Cg;Cas9>+;+;+ vs *Cg;Cas9>br-Z4 KO* | P0	1.0000
	Cg;Cas9>br KO *Cg;Cas9>br-Z4 KO* | P0	1.0000
defensin	*Cg;Cas9>+;+;+* vs *Cg;Cas9>br KO* | L3	0.6537
	Cg;Cas9>+;+;+ vs *Cg;Cas9>br-Z4 KO* | L3	1.0000
	Cg;Cas9>br KO *Cg;Cas9>br-Z4 KO* | L3	0.5756
	Cg;Cas9>+;+;+ vs *Cg;Cas9>br KO* | P0	0.2314
	Cg;Cas9>+;+;+ vs *Cg;Cas9>br-Z4 KO* | P0	0.0003
	Cg;Cas9>br KO *Cg;Cas9>br-Z4 KO* | P0	0.0831
metchnikowin	*Cg;Cas9>+;+;+* vs *Cg;Cas9>br KO* | L3	1.0000
	Cg;Cas9>+;+;+ vs *Cg;Cas9>br-Z4 KO* | L3	1.0000
	Cg;Cas9>br KO *Cg;Cas9>br-Z4 KO* | L3	0.7209
	Cg;Cas9>+;+;+ vs *Cg;Cas9>br KO* | P0	0.8651
	Cg;Cas9>+;+;+ vs *Cg;Cas9>br-Z4 KO* | P0	1.0000
	Cg;Cas9>br KO *Cg;Cas9>br-Z4 KO* | P0	0.4444

drs	*Cg;Cas9>+;+;+* vs *Cg;Cas9>br KO* | L3	1.0000
	Cg;Cas9>+;+;+ vs *Cg;Cas9>br-Z4 KO* | L3	1.0000
	Cg;Cas9>br KO *Cg;Cas9>br-Z4 KO* | L3	1.0000
	Cg;Cas9>+;+;+ vs *Cg;Cas9>br KO* | P0	<0.0001
	Cg;Cas9>+;+;+ vs *Cg;Cas9>br-Z4 KO* | P0	<0.0001
	Cg;Cas9>br KO *Cg;Cas9>br-Z4 KO* | P0	0.0002
drsl2	*Cg;Cas9>+;+;+* vs *Cg;Cas9>br KO* | L3	1.0000
	Cg;Cas9>+;+;+ vs *Cg;Cas9>br-Z4 KO* | L3	1.0000
	Cg;Cas9>br KO *Cg;Cas9>br-Z4 KO* | L3	1.0000
	Cg;Cas9>+;+;+ vs *Cg;Cas9>br KO* | P0	1.0000
	Cg;Cas9>+;+;+ vs *Cg;Cas9>br-Z4 KO* | P0	1.0000
	Cg;Cas9>br KO *Cg;Cas9>br-Z4 KO* | P0	1.0000
drsl3	*Cg;Cas9>+;+;+* vs *Cg;Cas9>br KO* | L3	1.0000
	Cg;Cas9>+;+;+ vs *Cg;Cas9>br-Z4 KO* | L3	1.0000
	Cg;Cas9>br KO *Cg;Cas9>br-Z4 KO* | L3	1.0000
	Cg;Cas9>+;+;+ vs *Cg;Cas9>br KO* | P0	1.0000
	Cg;Cas9>+;+;+ vs *Cg;Cas9>br-Z4 KO* | P0	0.9050
	Cg;Cas9>br KO *Cg;Cas9>br-Z4 KO* | P0	0.9168
drsl5	*Cg;Cas9>+;+;+* vs *Cg;Cas9>br KO* | L3	0.9520
	Cg;Cas9>+;+;+ vs *Cg;Cas9>br-Z4 KO* | L3	0.0167
	Cg;Cas9>br KO *Cg;Cas9>br-Z4 KO* | L3	0.2020
	Cg;Cas9>+;+;+ vs *Cg;Cas9>br KO* | P0	0.1613
	Cg;Cas9>+;+;+ vs *Cg;Cas9>br-Z4 KO* | P0	0.3062
	Cg;Cas9>+;+;+ *Cg;Cas9>br-Z4 KO* | P0	1.0000
Gene	**lsmeans, pairwise~Stage | Genotype**	**p-value**
cecropin A1	*Cg;Cas9>+;+;+* | L3 vs P0	<0.0001
	Cg;Cas9>br KO | L3 vs P0	<0.0001
	Cg;Cas9>br-Z4 KO | L3 vs P0	<0.0001
defensin	*Cg;Cas9>+;+;+* | L3 vs P0	<0.0001
	Cg;Cas9>br KO | L3 vs P0	<0.0001
	Cg;Cas9>br-Z4 KO | L3 vs P0	<0.0001
metchnikowin	*Cg;Cas9>+;+;+* | L3 vs P0	<0.0001
	Cg;Cas9>br KO | L3 vs P0	<0.0001
	Cg;Cas9>br-Z4 KO | L3 vs P0	<0.0001
drs	*Cg;Cas9>+;+;+* | L3 vs P0	<0.0001
	Cg;Cas9>br KO | L3 vs P0	0.0001
	Cg;Cas9>br-Z4 KO | L3 vs P0	0.4691
drsl2	*Cg;Cas9>+;+;+* | L3 vs P0	<0.0001
	Cg;Cas9>br KO | L3 vs P0	<0.0001

	Cg;Cas9>br-Z4 KO | L3 vs P0	<0.0001
drsl3	*Cg;Cas9>+;+;+* | L3 vs P0	<0.0001
	Cg;Cas9>br KO | L3 vs P0	<0.0001
	Cg;Cas9>br-Z4 KO | L3 vs P0	<0.0001
drsl5	*Cg;Cas9>+;+;+* | L3 vs P0	<0.0001
	Cg;Cas9>br KO | L3 vs P0	<0.0001
	Cg;Cas9>br-Z4 KO | L3 vs P0	<0.0001

S8 Table. Statistical analysis of AMP expression when *br* or *br-Z4* are knocked-out specifically in the fat body and haemocytes. lsmeans, pairwise~Genotype | Stage represents differences within the same stage, between genotypes. L3 is coloured in red and P0 in blue. lsmeans, pairwise~Stage | Genotype represents the difference between L3 and P0 within each genotype.

Primer name	***5'-Sequence-3' (Capital: gRNA sequences)***
br_common_PCR1_F01	cggcccgggttcgattcccggccgatgcaGGGGAGTTGGCAATATAGAGgtttcagagctatgctggaaac
br_common_PCR1_R01	TGGGCTCACCAATGCCAATCtgcaccagccgggaatcgaacc
br_common_PCR2_F01	GATTGGCATTGGTGAGCCCAgtttcagagctatgctggaaac
br_common_PCR2_R01	GCGAGGTGTGCGGTGCGACCtgcaccagccgggaatcgaacc
br_common_PCR3_F01	GGTCGCACCGCACACCTCGCgtttcagagctatgctggaaac
br_common_PCR3_R01	attttaacttgctatttctagctctaaaacCTGCCCACACATGACGTGTCtgcaccagccgggaatcgaacc
br_Z4_PCR1_F01	cggcccgggttcgattcccggccgatgcaGGAATTTATCTGGCTCTCATgtttcagagctatgctggaaac
br_Z4_PCR1_R01	CAACAACTAGACATGAACGCtgcaccagccgggaatcgaacc
br_Z4_PCR2_F01	GCGTTCATGTCTAGTTGTTGgtttcagagctatgctggaaac
br_Z4_PCR2_R01	CCTCCCGATCCACCCGCCGCtgcaccagccgggaatcgaacc
br_Z4_PCR3_F01	GCGGCGGGTGGATCGGGAGGgtttcagagctatgctggaaac
br_Z4_PCR3_R01	attttaacttgctatttctagctctaaaacCCGTACTCCTGTCCGCCTCCtgcaccagccgggaatcgaacc

S9 Table. 5'-3' sequences of primers used for tissue specific CRISPR. Guide RNA (gRNA) sequences are represented in capital letters.

Primer name	***5'-Sequence-3'***
rpl32 F01	CCAGTCGGATCGATATGCTAA
rpl32 R01	GTTCGATCCGTSACCGATGT
dif F01	CACAGTGGGCAACTCAAAAGTG
dif R01	GATGTCGTCCTTGGCAATCTTC
relish F01	ACAAAGGACGAGGATTCCGTGG
relish R01	TGATTCAGCAGCGAACAGAGCC
drosomycin F01	CTCTTCGCTGTCCTGATGCTGG
drosomycin R01	GACAGGTCTCGTTGTCCCAGAC
diptericin F01	TACTTTGGCTTATCCGATGCCC
diptericin R01	GTGCTGTCCATATCCTCCATTC
cecropin a1 F01	GTTTTCGTCGCTCTCATTCTGG
cecropin a1 R01	CTTGTTGAGCGATTCCCAGTC
defensin F01	TCGCTTTTGCTCTGCTTGCTTG
defensin R01	GTTGCAGTAGCCGCCTTTGAAC
metchnikowin F01	AGCGATTTTTCTGGCCCTGCTGG
metchnikowin R01	CTTGGTTGGTTAGGATTGAAGG
drsl2 F01	CCTGGCTGTGATGACAATTGTTG
drsl2 R01	ACTGATATGTCCCTCCTCCTTGC
drsl3 F01	TCCTAATGGAGGCCAACACTG
drsl3 R01	TCCCTCCTCAATGCAGAGACG
drsl5 F01	TCCTGGCTGTGATGACCATCTTC
drsl5 R01	ACTGGATCGTCCTTCCTCCTTG
br F01	CAATGCCAACGACGAACACAGCAA
br R01	ATTGGGAAAGTTGAAGGCGGCTG
Br-Z4 F01	GAACCACCACTCGTATTTCCAC
bR-Z4 R01	ACCGCCCACATTAACGCTATTG

S10 Table. 5'-3' sequences of primers used for qPCR